MASTERARBEIT | MASTER'S THESIS

Titel | Title

The regulation of adipose tissue loss during caloric restriction

verfasst von | submitted by

Filomena Sarra BSc

angestrebter akademischer Grad | in partial fulfilment of the requirements for the degree of

Magistra pharmaciae (Mag. pharm.)

Wien | Vienna, 2024

Studienkennzahl lt. Studienblatt | Degree programme code as it appears on the student record sheet:	UA 066 605
Studienrichtung lt. Studienblatt | Degree programme as it appears on the student record sheet:	Masterstudium Pharmazie
Betreut von | Supervisor:	Univ.-Prof. Dr. Jürgen König

Acknowledgement

First of all, I would like to thank Dr. Kalina Duszka very much for her patience and help. Above all, she believed in me, even if I was not really convinced that I could work in a laboratory again after so many years. Thank you for the encouragement and motivation.

Of course, my thanks also go to Univ.-Prof. Dr. Jürgen König and the entire laboratory that made it possible to work with you. Thank you Prof. Dr. Jürgen König for making it possible to end this project!

Thanks to Sandra Auernigg-Haselmaier, who showed me everything in the laboratory, learned the techniques and always had an answer to my questions.

I would also like to thank my laboratory colleagues Andrea Zöchling, Viktoria Blahova and Leonardo Gorza for their collaboration.

And a big thank you goes to my friend Sofia Skoulikari who was always there for me during this time of study!

But my biggest thanks go to my family, who have always supported me and who I want to show with this work that even if a lot of bad things happen, there are still beautiful moments in life! You are my strength and role model in this life. You should never give up and it is never too late to achieve something.

Vi voglio bene e sarete sempre la mia forza! Il mio GRAZIE non sarà mai abbastanza!

Tabel of content

Abbreviations

ACO1	Aconitase 1
ACO2	Aconitase 2
ACOT4	Acyl-CoA thioesterase 4
ACOX1	Acyl-CoA oxidase-1
ACOX2	Peroxisomal acyl-coenzyme A oxidase 2
ACSL3	Fatty acid CoA ligase Acsl3
Ad lib	Ad libitum
ADO	2-aminoethanethiol dioxygenase
BAT	Brown adipose tissue
BP	Blood pressure
BSH	Bile salt hydrolases
CDO	Cysteine dioxygenase type 1
CNP	Cardiac natriuretic peptide
Cpt1b	Carnitine palmitoyltransferase 1-b
Cpt1α	Carnitine palmitoyltransferase 1-α
CR	Calorie Restriction
DASH	Dietary Approaches to Stop Hypertension
E2	Estradiol
EBF2	Early B-Cell Factor-2
eWAT	Epididymal white adipose tissue
FAS	Fatty acid synthase
FMD	Fasting mimicking diet
FoxC2	Forkhead box protein C2
GSH	Glutathione
HDLc	High-density Lipoprotein cholesterol
HSL	Hormone-sensitive lipase
IF	Intermittent fasting
LDL	Low-density lipoproteins
LDLc	Low-density Lipoprotein cholesterol
LPL	Lipoprotein lipase
PAI-1	Plasminogen activator inhibitor-1
PGC-1α	Peroxisome proliferator-activated receptor gamma coactivator 1 alpha
PNPLA4	Patatin-like phospholipase domain-containing protein 4
PPARγ	Peroxisome proliferator-activated receptor gamma
PRDM16	PR domain containing 16
SNS	Sympathetic nervous system
SRC-1	Steroid receptor coactivator-1
TauT	Taurine transporter TauT
TFAM	Mitochondrial transcription factor A

TIF2	Transcriptional intermediary factor-2
UCP1	Uncoupling protein 1
UCP2	Uncoupling protein 2
VLDL	Very-low-density lipoprotein
WAT	White adipose tissue
β-3AR	β-3 adrenergic receptor

List of figures

List of tables

Abstract

Taurine has been proposed as a potential supplement to replicate the benefits of CR, and it is known that taurine supplementation influences lipid metabolism. Furthermore, in the study of Gregor et al., the authors observed that CR stimulates the synthesis, conjugation, secretion, and deconjugation of taurine and bile acids in the intestine, as well as their reuptake. In this study, we wanted to observe whether the CR-induced shift in taurine homeostasis contributes to adipose tissue loss.

This study aimed to observe and investigate fat mass loss of adipose tissue under caloric restriction. Particularly, we used different dietary approaches to obtain lower calorie intake based on the limitation either of carbohydrates or fat in various amounts of range. Since one of the major benefits of the CR diet is weight loss, we investigated this aspect wondering whether under specific dietary approaches we can stimulate the WAT browning process. In addition, we investigate the role of taurine by applying a low-taurine diet. Thus, we performed histological analysis of eWAT and BAT to visualize changes in the number, size, and dimensions of the adipocyte. Furthermore, the expression levels of genes involved in taurine transport (*e.g.* TauT), lipid metabolism *(e.g.* HSL), as well as involved in the browning process *(e.g.* UCP1). Finally, we further investigated concentrations of taurine and glutathione content in both eWAT and BAT tissue through the HPLC procedure.

In the current study, we performed multiple experiments assessing the mechanisms behind CR-trigger changes in taurine homeostasis. We demonstrated that CR WAT accumulates taurine in a higher manner compared to other tested tissues. Taurine concentration in WAT reversely correlated with eWAT weight. Cage bedding type revealed no significant changes in eWAT taurine levels; however, the absence of bedding in the cage indirectly affected taurine amounts. Supplementation of taurine accumulates taurine levels in eWAT, as well as in BAT, while reducing *Ad lib* mice's appetite. Finally, restriction of taurine or its precursors impaired fat loss during CR by affecting weight and taurine levels specifically in eWAT.

Zusammenfassung

Um die Vorteile von CR reproduzieren, wurde Taurin als potenzielles Supplement vorgeschlagen, da bekannt ist, dass eine Taurin-Zugabe den Lipidstoffwechsel beeinflusst. Darüber hinaus beobachteten die Autoren in der Studie von Gregor et al., dass CR die Synthese, Konjugation, Sekretion und Trennung von Taurin und Gallensäuren im Darm sowie deren Wiederaufnahme stimuliert. Wir wollten in dieser Studie untersuchen, ob die CR-induzierte Verschiebung der Taurin-Homöostase zum Verlust von Fettgewebe beiträgt.

Ziel dieser Studie war es, den Fettmassenverlust im Fettgewebe unter Kalorienrestriktion zu beobachten und zu untersuchen. Insbesondere verwendeten wir unterschiedliche Ernährungsansätze, um eine geringere Kalorienaufnahme zu erreichen, indem wir entweder Kohlenhydrate oder Fett in unterschiedlichen Mengen begrenzten. Da einer der Hauptvorteile der CR-Diät der Gewichtsverlust ist, haben wir diesen Aspekt untersucht und uns gefragt, ob wir mit bestimmten Ernährungsansätzen den WAT-Bräunungsprozess stimulieren können. Darüber hinaus untersuchen wir die Rolle von Taurin anhand einer taurinarmen Ernährung. Daher führten wir eine histologische Analyse von eWAT und BAT durch, um Veränderungen in der Anzahl, Größe und Dimension der Adipozyten sichtbar zu machen. Darüber hinaus wurden die Expressionsniveaus von Genen, die am Taurintransport (z. B. TauT), am Lipidstoffwechsel (z. B. HSL) sowie am Bräunungsprozess beteiligt sind (z. B. UCP1), ermittelt. Schließlich untersuchten wir die Konzentrationen des Taurin- und Glutathiongehalts sowohl im eWAT- als auch im BAT-Gewebe mithilfe des HPLC-Verfahrens weiter.

In der aktuellen Studie haben wir mehrere Experimente durchgeführt, um die Mechanismen hinter CR-auslösenden Veränderungen in der Taurinhomöostase zu untersuchen. Wir haben gezeigt, dass CR WAT im Vergleich zu anderen getesteten Geweben Taurin stärker anreichert. Die Taurinkonzentration im WAT korrelierte umgekehrt mit dem eWAT-Gewicht. Die Art der Käfigeinstreu zeigte keine signifikanten Veränderungen im eWAT-Taurinspiegel. Das Fehlen von Einstreu im Käfig wirkte sich jedoch indirekt auf die Taurinmenge aus. Durch die Ergänzung mit Taurin wird der Taurinspiegel sowohl im eWAT als auch im BAT erhöht und gleichzeitig der Appetit von *Ad-lib*-Mäusen reduziert. Schließlich beeinträchtigte die Einschränkung von Taurin oder seinen Vorläufern den Fettabbau während der CR, indem sie sich speziell auf das Gewicht und den Taurinspiegel im eWAT auswirkte.

1. Introduction

1.1 Diet and Calorie Restriction (CR)

In the past years, we have witnessed a special interest of global society in maintaining health span and longevity through adequate nutrition, which can also prevent disease and improve quality of life [1]. Good nutrition requires the right amount of macronutrient consumption (carbohydrates, proteins, and fats), necessary to support cellular processes.

As the primary source of energy, carbohydrates are found in abundance in grains, legumes, vegetables, as well as fruits. Protein is another source of energy and it is a fundamental source of amino acids, specifically for those that are not produced in the human body (*e.g.* essential amino acids) [1].

Different dietary approaches have been analyzed through epidemiological studies; however, more and more studies have been conducted specifically on how nutritional approaches can reduce the onset and incidence risk of multiple diseases, such as the Dietary Approaches to Stop Hypertension (DASH) [1]. Moreover, clinical finding suggests that an additional dietary intervention as a support of drug-therapy positively enhances patient health span that suffers from *e.g.* cancer, obesity, and Alzheimer disease [1]. Thus, the final aim of dietary studies is to develop individualized nutritional therapy based on patient requirements, pathology, or age [2].

Calorie restriction (CR) is a dietary intervention that relies on the reduction of energy intake by 20-50%, without malnutrition. Positive effects of CR regimens on lifespan were demonstrated already in 1935 in rats; however, additional recent discoveries suggested that the improvements observed in animal models can be translated to humans [2, 3]. For instance, moderate CR enhances metabolic and hormonal factors involved in the pathogenesis of metabolic disease and cancer [3, 4]. In addition, moderate CR can prevent and reverse the negative effects of the accumulation of excessive body fat [4]. Furthermore, CR showed remarkable benefits for health in both human and animal models by lowering the incidence of several metabolic diseases [5].

The metabolic adaptation to CR includes a broad spectrum of pathways, resulting in multiple phenotype outcomes such as reduction of inflammation, metabolic rate, body temperature, fat metabolism, and insulin sensitivity [5]. CR duration can vary from short-term interventions to a few weeks of treatment [6].

1.2 Calorie restriction benefits

Calorie restriction has been intensively investigated and adopted for weight loss. For instance, Kraus et al. demonstrate that over 2 years of CR, healthy men and women reduced their body weight, of which the majority was fat mass loss, compared to the control group [7]. However, there are multiple difficulties regarding the CR diets, since not all patients are physically and psychologically able to adhere to a long-term CR approach [8]. At the beginning of the CR-based studies, the primary outcome observed in the CR diet was the reduction of total calorie intake; so, the phenotype was independent of the daily intake of either macro or micro-nutrients. However, recent discoveries suggest that the reduction of specific macronutrients (principally carbohydrates and fats) might show the same effects observed under the CR regime [8].

The benefits achieved by CR regime are observed because the calorie reduction influences energy metabolism. Indeed, nutrient restriction in mice and flies has shown an upregulation in both the synthesis and catabolism of fats [2]. CR approach increases mono and poly-unsaturated fatty acids, promoting survival cell mechanisms [2]. Studies conducted in mice on CR regiments demonstrated an increased expression of genes involved in fatty acid oxidation and, on the other hand, a decreased one in fatty acid synthesis, compared to *ad libitum* (*ad lib*) fed controls [9].

Despite the interesting studies regarding CR and its benefits on healthy and diseased patients, the complexity of pathways involved in the response and the molecular mechanisms behind CR are still poorly understood.

1.3 Carbohydrates and CR

Carbohydrates, commonly called sugars, are the main source of energy.

They are divided into:

• Monosaccharides: characterized by a simple structure: glucose, fructose and galactose

• Disaccharides: formed by two monosaccharides such as sucrose, lactose and maltose.

• Oligosaccharides: composed of two to ten molecules of monosaccharides such as maltodextrin often used as energy supplement.

Hexoses, made up of six carbon atoms, are the most important component of diets, especially glucose: the form in which sugars must be transformed to be used by our body.

Complex carbohydrates or polysaccharides (made up of ten to thousands molecules of monosaccharides) are distinguished by their animal origin (glycogen: reserve of carbohydrates in the muscle) and vegetables (starches and fibers) [10].

When low-carb diets were first proposed, they were mostly studied in the treatment of epilepsy. So as more data points to their efficacy in treating a variety of different medical illnesses, such as diabetes, neoplasms, gastrointestinal, lung disorders, cardiovascular issues, and obesity, their potential uses have grown. Diets low in carbohydrates have become more and more popular as a means of losing weight, and nutritionists are still interested in them. However, there are negative consequences associated with high and low carbohydrate intake. Because the increased energy from carbohydrate intake causes obesity, and excessive glucose intake causes lipogenesis [11].

1.4 Proteins and CR

Proteins are made up of simple molecules called amino acids; we have 20 different amino acids and they can bind together forming chains.

The amino acids are divided into essential: which cannot be synthesized by our organism and must be introduced through food, and non-essential: those that can be synthesized by our organism in adequate quantities.

The biological functions of proteins in the organism are:

- Regulatory function: they control many processes of the organism, in the form of enzymes and hormones;
- Building function: they allow us to grow and maintain the structures of our body;
- Blood transport function: some of them transport nutrients and other substances in the blood (for example lipoproteins transport fats and hemoglobin oxygen);
- Immune defense function: antibodies are proteins responsible for the defense of our organism;
- Energy function: a small percentage of proteins is daily used for energy purposes, this amount tends to increase with physical exercise;
- Defense function from external agents: so keratin is the protein in nails and hair, which protects delicate areas [10].

High-protein diets have become more and more popular as a weight-loss strategy in the last few years. However, questions have been raised about the safety of diets high in protein. These dangers include liver, bone, kidney, cardiac, and metabolic disorders. One of the main issues with low-carb, high-protein diets is the potential for metabolic ketosis. Reduced carbohydrate intake causes the body to switch to using fat as its energy source. Increased ketone body production and release into the bloodstream may follow from this. An imbalance in the body's acid-base balances, known as metabolic acidosis, can result from elevated ketone body levels. Severe occurrences of this illness may result in a coma or even death. Diets high in protein may have detrimental effects on blood pressure and blood lipid profiles, raising the risk of cardiovascular disease. The main cause of these consequences is the increased consumption of saturated fats, which is frequently linked to these kinds of diets [12].

1.5 Metabolism and synthesis of lipids

As mentioned before, macronutrients are fundamental to supplying the body with all the physiological energy requests. Carbohydrates play a major role as the primary source of energy, while protein intake is necessary to keep a lean body mass throughout the life span and is a fundamental supplier of amino acids. Fats are also another source of energy, and in addition, fats are the primary structural building blocks of cellular membranes [1]. An excess of dietary carbohydrates led to this macronutrient conversion into triglycerides through the synthesis of fatty acids from acetyl-CoA in a process called lipogenesis. Dietary fats are classified based on the number of double bonds they possess: thus, we can distinguish saturated, monounsaturated, polyunsaturated, and trans fats.

Lipid metabolism of dietary fats can be subdivided into three main processes, involving a broad series of several cells and enzymes, and will be briefly explained as follows:

1. **Digestion**: starts in the mouth and consists of the breakdown through lipase of the triglycerides into monoglyceride. Digestion is continued in the stomach by gastric lipase and peristalsis. However, lipid digestion and absorption occur in the small intestines due to the secretion of pancreatic lipases by the pancreas. The digestion part is fundamental to allow the diffusion of these smaller units in the small intestine [13];
2. **Absorption**: in this process, the units of fatty acids and glycerols enter the intestinal epithelial cells by diffusion. Here, they are recombined into triglycerides, and packed into chylomicrons. This specific structure allows the transport of lipids through the bloodstream to other tissues, such as the adipose tissue [13];
3. **Transportation**: the chylomicron's densities depend on the types of lipoproteins and fats they transport. Very-low-density lipoproteins (VLDL) are formed by triglycerides synthesized by the liver, while on the other hand low-density lipoproteins (LDL) transport the cholesterol [13];
4. Finally, the majority of the lipids are stored in white adipose tissue as triglycerides, or transported to other tissues in a lower percentage.

In addition to being absorbed from food, fats can be synthesized through lipogenesis by the liver [14]. Based on the kind of lipid synthesized, four main biochemical processes can be distinguished:

1. Membrane lipid biosynthesis: this process occurs in the endoplasmic reticulum membrane. The first step consists of the synthesis of the backbone, followed by the addition of fatty acids, and finally with the attachment of different hydrophilic head groups [13], which characterize the type of lipid.
2. Triglyceride biosynthesis: this process occurs in the cytosol. In this pathway, the phosphatidic acid will be converted into triglycerides by acyltransferase through the diacylglyceride intermediate [13].
3. Fatty acid biosynthesis: this process occurs in the cytoplasm as well, and it starts with acetyl-CoA as a precursor [13].

When stored fat is required to fulfill the energy requests from the body, triglyceride will be broken down by hydrolysis to fatty acid in a process called lipolysis. Hormone-sensitive lipase (HSL) is the hydrolase with higher activity against diacylglycerol and cholesterol esters [14]. Fatty acids constantly migrate through adipose tissue generating a flux controlled by the antagonist action of insulin and leptin hormone levels. For instance, low insulin levels lead fatty acids to leave the adipose tissue [15]. Despite fatty acids act as metabolic substrates, their excess leads to the accumulation of toxic lipids with a negative and harmful effect, and this lipotoxicity has been linked to multiple processes like inflammation and insulin resistance [14].

1.6 Adipose and fat tissue: eWAT and BAT

Two different types of adipose tissue can be distinguished: white adipose tissue (WAT) and brown adipose tissue (BAT). While WAT stores energy as triglycerides, BAT specializes in the dissipation of energy from stored fat as heat. In addition, adipose tissue secretes protein hormones involved in energy metabolism, such as leptin, resistin, estradiol (E2), and Plasminogen activator inhibitor-1 (PAI-1) [16]. WAT and BAT differ not only in their antagonizing functions but also in the shape and morphology of their adipocytes [16]. Since

the main function of BAT is to dissipate energy to produce heat, this tissue is found abundant in small mammals or newborns, which are naturally predisposed to temperature loss [17]. Adipocytes are distributed in multiple body regions called adipose depots. Adult human BAT composition changes throughout life, and it is mostly distributed throughout the cervical, supraclavicular, axillary, paravertebral, mediastinal, and upper abdominal regions [17]. On the other hand, WAT is found to be distributed as subcutaneous fat, the primary type of WAT in the body, and as visceral WAT, which surrounds the inner organs. The visceral fat has a more harmful significance since its excess has been linked to poor insulin sensitivity, type II diabetes, and

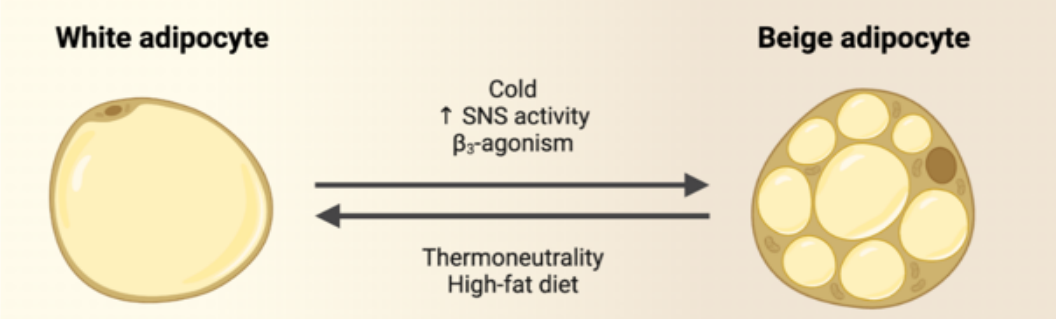

Figure 1.1 - Adipocyte differences in the browning process: low temperature, activation of the sympathetic nervous system (SNS), or β_3-AR binding molecules. The process is reversible, and a high-fat diet increases the amount of WAT tissue. *Figure readaptet from Demine, Renard, & Arnould (2019) [24]; Ro, S.-H., Jang, Y., Bae, J., Kim, I. M., Schaecher, C., & Shomo, Z. D. (2019) [25]; from BioRender 2020 template.*

obesity-related diseases. Multiple adipose depots comprise the visceral fat, such as mesenteric, epididymal white adipose tissue (eWAT), and perineral depots [17]. BAT generates heat through a process in which the respiratory chain of oxidative phosphorylation is uncoupled within mitochondria by the expression of uncoupling protein 1 (UCP1), which is activated by multiple factors, primarily by cold exposure [18]. Particularly, BAT activation increases energy expenditure and decreases metabolic efficiency, and this process has been shown to positively affect triglyceride and cholesterol levels, glucose tolerance, insulin sensitivity, and weight loss [18]. Pivotal studies demonstrate that under specific conditions WAT can change to BAT-like adipocytes. Both pharmacological and dietary approaches have been established to manipulate and increase the amount of brown fat in a process called browning [19]. Among the endogenous stimuli, the browning process can be activated by cold, food intake, thyroid hormones, and training [19]. However, the effectors behind the

selective molecular mechanism that leads to browning are still the object of numerous studies. As mentioned before one of the primary stimuli of WAT browning is cold exposure, but also exercise training activates the browning process by targeting visceral and subcutaneous WAT [20]. β-3 adrenergic receptor (β-3AR) appears to be the mediator of tissue thermogenesis-response inducing WAT browning [19].

For instance, noradrenaline and adrenaline stimulation directly affect lipolysis after binding β-3AR localized on the fat cell surface. This interaction led to a cascade of signals that ended with the overexpression of proteins involved in thermogenic homeostasis like UCP-1 [18]. Moreover, one of the major effectors mediating the thermogenesis-variation response is the activation of the sympathetic nervous system (SNS) [21].

Among the molecular factors involved in the browning process, transcriptional regulators have been proposed, such as peroxisome proliferator-activated receptor gamma coactivator 1 alpha (PGC-1α), peroxisome proliferator-activated receptor gamma (PPARγ), Early B-Cell Factor-2 (EBF2), as well as PR domain containing 16 (PRDM16) [22-23]. Finally, other transcription factors and coregulators are emerging as effectors of the browning process: forkhead box protein C2 (FoxC2), steroid receptor coactivator-1 (SRC-1), transcriptional intermediary factor-2 (TIF2), mitochondrial transcription factor A (TFAM), as well as secreted proteins like cardiac natriuretic peptide (CNP), or FGF21, for instance [24].

Finally, WAT browning can be stimulated by intermittent fasting or low protein/high carbohydrate diets [25]. For instance, Fabbiano et al. [22] observed that long-term CR as well as intermittent fasting, stimulate WAT browning.

In conclusion, the number of factors involved in the browning process is continuously expanding and it is still an interesting research subject. The deep knowledge achieved during the last years of the molecular mechanism behind the WAT browning would thus allow the creation of a therapy that selectively induces the browning process for specific disorders (*e.g.* obesity).

1.7 Taurine and its effects

Taurine (2-aminoethanesulfonic acid) is a free-amino acid not used in protein synthesis. Different studies underlined taurine contribution to biological processes such as anti-oxidation, anti-inflammation, cell membrane stabilization, and neuromodulation [26]. Despite taurine can be found in different amounts in several mammalian tissues, it is not an essential human nutrient [27]. Taurine occurs naturally in fish and meat, while it is found in only low or almost absent concentrations in vegetables. Taurine is synthesized in the liver, controlled by the metabolic process that relies on cysteine/methionine primary substrates, taurine-producing enzymes cysteine dioxygenase, cysteine sulfinate decarboxylase, and taurine transporter (TauT) [27]. However, another study in rats suggests that taurine might be also synthetized in the epididymal and perirenal white adipose tissues [28]. Taurine localizes into mitochondria rather than cytosol, which plays a role in various mitochondrial processes such as energy metabolism, thermogenesis, and oxidation of fatty acids [27]. It has been reported in multiple studies that taurine stimulates fatty acid oxidation through AMPK-PPARα pathway, indirectly affecting thus various factors such as aconitase 1 (ACO1), aconitase 2 (ACO2), hormone-sensitive lipase (HSL), lipoprotein lipase (LPL), acyl-CoA oxidase-1 (ACOX1), and carnitine palmitoyltransferase 1-α (Cpt1α) [27].

More evidence linked dietary taurine to lipid and glucose metabolism, as well as energy control homeostasis. For instance, in the study by Cao et al., the authors observed that taurine intake may stimulate energy release, mostly fatty acid β-oxidation in adipose tissue, improving weight loss in an obese mice-model [26]. Furthermore, studies in mice demonstrate that taurine is involved in the adaptive thermogenesis response that led to the browning of inguinal white adipose tissue by activating a cascade signal involving the activation of uncoupling protein 1 (UCP1) [27].

On the other hand, it has been reported that taurine depletion negatively affects adipocyte metabolism [27]. After intraperitoneal glucose injection, in the same study, the authors observed an increase in blood glucose disposal rate with a diminished serum insulin one, suggesting a reduced activation in adipose tissue [30].

1.8 Aim of the study

The aim of this study was to observe and investigate fat mass loss of adipose tissue under caloric restriction. Particularly, we used different dietary approaches to obtain lower calorie intake based on the restriction either of carbohydrates or fat. Since one of the major benefits of the CR diet is weight loss, we investigated this aspect wondering whether under specific dietary approaches, we can stimulate the WAT browning process. In addition, we investigate the role of taurine in the process by a low-taurine diet approach. Thus, we first observed the tissue for both eWAT and BAT histologically by microscopy, to investigate visible changes in the number, size, and dimensions of the adipocyte. Furthermore, the expression levels of genes involved in taurine metabolism (*e.g.* TauT), genes known to code proteins for lipid metabolism (*e.g.* HSL), as well as genes involved specifically in the browning process (*e.g.* UCP1) were measured. Finally, we further investigated concentrations of taurine and glutathione release in both eWAT and BAT tissue by HPLC.

2. Material

2.1 Equipment

- Centrifuges: 5418R, 100-14 000 rpm, 0-40°C, Eppendorf Ltd (Hamburg, Germany); Thermo Scientific™ Megafuge™ 8, Fisher Scientific GmbH (Schwerte Germany)
- Tubes: 15 ml, 50 ml, Corning Ltd (Corning, New York, USA)
- Microcentrifuge tubes: 1.5ml and 2ml; Eppendorf Austria GmbH (Vienna, Austria)
- Pipette: 2,5, 10, 100, 200, 1000 µl; Eppendorf Reference® 2; Eppendorf
- Tips: 0.1 - 20 µL, 10 - 100 µl, 100 -1 000 µl, epT.I.P.S.® 384; Eppendorf
- Block heater: SBH130D, SBH200D Stuart® via BioCote; Liebisch Labtherm 2009 Digital; Thermostat 5320 Dry Bath Heat Block (Eppendorf Netheler-Hinz GmbH Hamburg, Germany);
- Vortex mixer, lab dancer, VWR® International Ltd (Radnor, USA).
- Rocker – Shaker Fisherbrand Sea Star; Fisher Scientific GmbH (Schwerte Germany).

2.2 Quantitative Real-Time PCR (qRT-PCR) material

For RNA-extraction and cDNA synthesis procedure:

- RNAkit: peqGOLD HP RNA kit; peQlab; VWR International GmbH (Erlangen);
- Precellys shaker: Homogenisator, Precellys© 24; VWR;
- NanoDrop™ One/OneC Microvolume UV-Vis Spectrophotometer; ThermoFisher Scientific;
- cDNA kit: First strand cDNA synthesis kit, VitaScript, PROCOMCURE Biotech GmbH;

For qPCR reaction:

- Dispenser 0.5-10µL, 5-100µl, Eppendorf Xplorer®, (Hamburg, Germany);
- qPCR seal 4titude® via Brooks Life Science
- Frame Star® 384 Well Skirted PCR Plate, Roche Style; 4titude® via Brooks Life Science
- CFX Connect Real-Time PCR Detection System, Bio-Rad Laboratories Ltd. (Hercules, USA)

2.3 Histology materials

For embedding:

- Embedding station AP 250 W, Microm Ltd (Walldorf, Germany);
- Histology cassettes, VWR® International Ltd (Radnor, USA);
- Peltier-cooled incubator IPP110, VWR® International Ltd (Radnor, USA)

For histological sectioning:

- Low Profile Microtome Blades DB80 LS, Leica Biosystems Ltd (Nussloch, Germany);
- Microscope slides Superfrost® Plus, Thermo Scientific Ltd (Braunschweig, Germany);
- Slide holders, VWR® International Ltd (Radnor, USA);
- Slide boxes (100 lame) VWR® International Ltd (Radnor, USA);
- GFL Paraffin stretching bath (1052), Lauda-GFL Ltd (Burgwedel, Germany);
- Semi-motorized rotary microtome (RM2245), Leica Biosystems Ltd (Nussloch, Germany).

2.3.1 Stainings

- Dyeing troughs for manual dyers, VWR® International Ltd (Radnor, USA);
- Stainless steel caps for dyeing troughs, VWR® International Ltd (Radnor, USA);
- Micro cover glasses (20x20 mm);

2.3.2 Microscopes

- Axiocam ERc 5s, Carl Zeiss Microscopy Ltd (Göttingen, Germany);
- Axio Lab 5x H SF 22, Carl Zeiss Microscopy Ltd (Göttingen, Germany).

2.4 Mass Spectrometry (MS) and High-performance liquid chromatography (HPLC)

- vials 2 ml; Sigma-Aldrich Chemie GmbH;
- Precellys tubes: Fisherbrand™ Free-Standing Microcentrifuge Tubes with Screw Caps;
- Precellys shaker: Homogenisator, Precellys© 24; VWR.

2.5 Softwares

- ImageJ
- Zeiss efficient Navigation Software Program (ZEN)
- Applied biosystems®, Quant studioTM 6 Flex Real-time PCR System, OptiFlexTM Optics System; Life Technologies Holding (Singapore)
- Microsoft Office

3. Reagents

3.1 Histology Reagents

- ddH2O, produced in the lab with Arium®pro
- Eosin Y disodium salt ≥85%, Sigma Aldrich Ltd. (Steinheim, Germany)
- Ethanol ≥96%, 80%, 70%, 30%
- Eukitt® Quick-hardening mounting medium for microscopy, Sigma Aldrich Ltd. (Steinheim, Germany)
- Mayer's hematoxylin solution (Gill No.2), Sigma Aldrich Ltd. (Steinheim, Germany)
- Xylene, histological grade, Sigma Aldrich Ltd. (Steinheim, Germany)

3.2 HPLC/MS solvents

- ROTISOLV HPLC gradient grade water + 0.1% formic acid (Solvent A);
- ROTISOLV HPLC gradient grade acetonitrile + 0.1% formic acid (Solvent B);
- ROTISOLV gradient grade HPLC Water;
- Methanol: ROTISOLV® HPLC Gradient Grade; ROTH
- Acetonitrile: ROTISOLV® HPLC Gradient Grade; ROTH
- Formic acid: ROTIPURAN® ≥ 98 %, p.a., ACS; ROTH
- Taurine, Sigma Aldrich
- Glutathione, Sigma Aldrich

3.3 qPCR reagents

For RNA extraction:

- Chloroform
- EtOH 100%
- EtOH 70% in sterile DEPC-dH_2O

For RNA precipitation:

- NaAc 10%
- EtOH 100% - 75%
- RNAse-free water

For qPCR reaction:

- SYBR Green qPCR Master Mix, CharmQ Universal Q711-02; Vazyme (Nanjing, PCR)
- Primers (foward and reverse):

Table 3.1 – qPCR primers and gene sequences

Gene name	Gene sequence
Eef1α1	fw: CCTGGCAAGCCCATGTGT rv: TCATGTCACGAACAGCAAAGC
HSL	rv: TCCACTTAGTTCCAGGAAGGAGTTC fw: TCAGGGACAGAGGCAGAGGAC
FAS	fw: CAGAAATCGCCTATGGTTGTTG rv: GCTCAGCTGTGTCTTGGATGC
ACOT4	fw: TGCGGTATGCTTCGACAT rv: TGGAAACTGTGGCTGAGACAT
ACOX2	fw: GCCTCATGCAATACTCTGGC rv: GGTACCAAGAACCTCTGTCCTG
ACSL3	fw: GAGCCCGCGGTTATTCTGG rv: CCAAAGTCAAGGGCTCGGAT
UCP2	fw: CAGTTCTACACCAAGGGCTCAGAG rv: TGACAATGGCATTACGGGAACAT
PPARγ	fw: TGCCTATGAGCACTTCACAAGAAAT rv: CGAAGTTGGTGGGCCAGAA
ADO	fw: GGTCACCTACATGCACATCTACG rv: ACAGCACCTTGAGCATACCGT
Cpt1b	rv: CCTGGGATGCGTGTAGTG fw: ATGTATCGCCCGCAAACTG
UCP1	fw: CACCTTCCCGCTGGACACT rv: TCGGCAATCCTTCTGTTT
PNPLA4	fw: CGAGGCGAGCGGTACGT rv: TGACACCGTGATGGTGGTTT
TFAM	rv: CGAATCCTATCATCTTTAGCAAGC fw: GAGGCAAAGGATGATTCGGCTC
PGC-1α	fw: GCGTCATTCGGGAGCTGGAT rv: CCAACCAGAGCAGCACACTCT
CDO	fw: GGGGACGAATCAACGTGG rv: ACCCCAGCACAGAATCATCAG
TauT	rv: ATTTTTGTAGCAGAGGTACGGG fw: GCACACGGCCTGAAGATGA

4. Methods

4.1 Mice treatment and bedding

To better understand the role of calorie restriction on adipose tissue loss, multiple treatments were performed. Generally, in all the experiments mice were divided into groups, comprising 8 mice per group. All the experiments lasted 14 days. In some conditions, mice were also treated under *ad libitum* conditions, meaning that there are no restrictions on the amount or frequency of consumption [31].

To explore taurine effects on adipose tissue and its role in calorie restriction, a low-taurine nutritional approach was followed in *ad libitum* condition (*Ad lib* LTD) or under calorie restriction (CR LTD), compared to group of mice under calorie restriction (CR). As a control, an *ad libitum*-fed group of mice was used (*Ad lib* Ctrl). Both eWAT and BAT were analyzed under the aforementioned dietary intervention by histological, qPCR and HPLC approaches. The amount of taurine in the low-taurine diet approach is summarized in Table 4.1.

Table 4.1 - Taurine amount during mice feeding

g/100g	**Low-taurine diet (LTD)**	**Normal-taurine diet (NTD)**
Casein	10	10
Cornstarch	52,3	51,8
Sucrose	10	10
Maltodextrin	12,5	12,5
Soybean oil	5	5
fibre mix	3	3
vitamin mix w/o choline	1	1
mineral mix	6	6
Choline	0,2	0,2
Taurine	**0**	**0,5**
L-cysteine	0	0

Furthermore, to investigate how the reduction of a specific macronutrient diet might affect white adipose tissue, mice were divided into 5 groups, and the adipose tissue was analyzed under microscopy. The four nutritional reductions with the respective amount are summarized in table 4.2, and compared to the custom-made control group of mice.

Table 4.2 - Mice macronutrient restriction intervention

g/100g	Control	Low-fat	Low-carbohydrate	Very low-carbohydrate	Very low-fat
Casein	5,8	9	15	20	9
Soy protein	5,8	9	15	18	9
Whey protein	5,8	9	15	18,21	9
L-cysteine	0,18	0,18	0,18	0,18	0,18
Corn starch	43,22	37,67	12,41	6	38,07
Maltodextrin 10	12	12,5	10	1	12,5
Sucrose	9	10	6	4	10
Cellulose	4	4	4	4	4
Inulin	1	1	1	1	1
Soybean oil	0,5	0,1	5,31	6,81	0
Beef tallow	2,5	0,1	1,77	3,37	0
Olive oil	0,5	0,1	5,31	6,81	0,1
Coconut oil	2,5	0,1	1,77	3,37	0
Minerals	6	6	6	6	6
Vitamins	1	1	1	1	1
Choline	0,2	0,25	0,25	0,25	0,25

Each group of mice was treated with a reduction of different percentages on either fat or carbohydrate amounts, leading thus to a different type of diet based on the decreased intake of a specific macronutrient (low or very-low fat, low or very-low carbohydrates), which is shown in table 4.3.

Table 4.3 - Percentages of macronutrient intake during different nutrient restriction

(En%)	Control	Low-fat	Low-carbohydrate	Very low-carbohydrate	Very low-fat
Protein	18	31	43	50	31
Fat	14	1	30	40	0
Carbo	67	68	27	10	69

Finally, calorie restriction intervention was then investigated with or without bedding. Thus, CR regime and *ad libitum* control were then performed with or without bedding. Both eWAT and BAT composition were analyzed by histology approach, as well as the expression of genes was investigated by qPCR.

4.2 Histological tissue methods

4.2.1 Tissue preparation and embedding

Histological samples from adipose tissue were placed in histological cassettes and incubated for 48h in 4% formalin/PBS solution. At the end of the incubation time, the samples were washed and rinsed under running cold tap water for 15 minutes and stored for at least 1h in a 75% ethanol solution. Afterward, the samples were incubated for 1h at room temperature in 85% ethanol under shaking. The samples were then stored overnight in 95% ethanol + 5% methanol in a cold room. The day after, the samples were washed three times with absolute ethanol for 1h under shaking. The samples were incubated twice in xylene for 45 minutes each. The paraffin was previously melted at 60 °C; thus, the melted paraffin was heated at 60 °C and labeled as Paraffin I, Paraffin II, and Paraffin III. Each of these paraffins was added to the samples for 30 minutes at 60 °C in the incubator. Between every paraffin step, the samples were shaken every 5 minutes. After the last paraffin incubation, the samples were then embedded in paraffin through the embedding machine. Thus, samples were divided into multiple sections. The tissue blocks were released from the embedding machine and led to solidification in a specific position. The tissue blocks were then stored in the cool room until the cutting process.

4.2.2 Tissue sections cutting

The embedded tissue samples were cooled at –20 °C for at least 10 minutes before the sectioning. To avoid paraffin sample contamination and approach better the sample in the next step, the excess of paraffin is trimmed away by setting in the machine the thickness of the slice as 16 µm with the "TRIM" function. Once close to the tissue, the tissue blocks were cut into sections of 4°µm thickness with the "SECT" function in the machine. Three sections are taken from each sample, corresponding typically to 1-2 sections per slide. The cut sections were then transferred to a water bath and mounted on slides. Finally, the slides were left to dry for 48-72 hours at 37 °C.

4.2.3 Hematoxylin and Eosin staining

The tissue samples were first dehydrated by xylene for 20 minutes, followed by multiple dehydration steps with ethanol at different percentages (20 min x 95% EtOH, 10 min x 85% EtOH, 10 min x 70% EtOH, and 10 min x 30% EtOH). All these dehydration steps were performed under gentle shaking to achieve better penetration of the solutions. Next, the samples were deeply rinsed with distilled water two times for 10 min. All the samples were then stained with hematoxylin for 1 min and rinsed two times in running tap water for 30 s. Next, samples were rinsed in distilled water for 10 min. Before the eosin staining, the samples were dehydrogenated two times for 8 min in 70% ethanol and 85% ethanol, respectively. Finally, the samples were counterstained in eosin for 1-2 s (BAT) or 4-5 s (eWAT), and dehydrated again for 10-20 s in previously used 95% and fresh 95% ethanol. Afterward, the samples were then immersed in xylene for 20 min, and then the slide bottom was wiped with a piece of paper. In the last step, the slides were mounted with a drop of Entellan on the coverslips and left to air-dry.

4.2.4 Microscopy

To facilitate further analysis, images of the samples were captured at both 10x and 20x magnification by Axio Lab Microscopy (see 2.3.2). Pictures were then analysed with ImageJ.

4.3 qPCR sample preparation

4.3.1 Total RNA isolation

Tissue samples were disrupted in 200 µl per 10 mg tissue by homogenization through a homogenizer. Then, the samples were kept for 5 minutes at room temperature to allow the dissociation of the nucleoprotein complexes. After adding 40 µl of chloroform per 1 mL of peqGOLD TriFast^{TM}, the samples were shaken by hand for 15 s and kept for 3-10 minutes at room temperature. The samples were then centrifuged at 12.000 x g for 5 minutes to allow the mixture separation into lower red-colored (phenol-chloroform), interphase (containing DNA and proteins), and colorless aqueous upper phase, where the RNA is exclusively forced. The RNA-containing aqueous upper phase was transferred into a new 1.5 ml sterile centrifuge tube. 70% EtOH equal volume of the lysate was added to each sample and vortexed. The samples were added to the PerfectBind RNA Column which was previously placed in a 2 mL Collection Tube. The PerfectBind RNA Column with the Collection Tube assembly was then centrifuged at 10.000 x g for 60 sec, and the flow-through from the collection tube was removed. To wash the membrane, 500 µl RNA Wash Buffer I was added to the PerfectBind RNA Column and centrifuged for 60 sec at 10.000 x g. Then, the PerfectBind RNA Column containing the RNA in the membrane was placed in a new Collection Tube, and the flow-throw was discarded. 600 µl RNA Wash Buffer II was added to the PerfectBind RNA Column to wash the membrane and centrifuged for 60 sec at 10.000 x g. This washing step was repeated another time. Afterwards, the PerfectBind RNA Column was placed in a new Collection Tube and centrifuged for 60 sec at 10.000 x g to dry the membrane. In the final step, the PerfectBind RNA Column was placed into a 1.5 ml microcentrifuge tube, and RNA in the matrix was eluted by adding 30 µl of sterile RNase-free Water and centrifuged for 60 s at 10.000

x g. The filtrate was then re-loaded onto the membrane to better allow RNA dissociation from the PerfectBind RNA Column and increase the RNA concentration. Finally, the RNA concentration was measured by NanoDrop spectrophotometer. When the samples showed A260/230 lower than 1.5 value, the RNA was precipitated as described in the next subchapter.

4.3.1 RNA precipitation

For RNA precipitation, 30 µl of each sample was added 3µl 10% NaAc and 90 µl absolute EtOH (cold), followed by vortexing. Afterwards, the samples were incubated at –20 °C for a minimum of 3h, and then centrifuged for 30 min 12.000 x g at 4 °C. The EtOH was emptied, and then 90 µl cold EtOH 75% was added to the samples. After vortexing, the samples were centrifugated for 15 min 12.000 x g at 4°C. EtOH was again emptied by brief evaporation and the remaining EtOH was carefully removed by pipetting. The precipitated RNA was solved in 30 µl free-RNAse water, vortexed, and briefly centrifuged for 10 s. RNA concentrations were then measured by NanoDrop, using RNAse-free water as a blank value.

4.3.2 cDNA synthesis

For cDNA synthesis, the VitaScript First Strand kit was used and the reverse-transcriptase mix was prepared by following the manufacturer's instructions (table 4.4).

Table 4.4 – VitaScript master mix preparation cDNA synthesis

Ingredients	Volume (µl)
5X VS Reaction Buffer	4
VitaScript Enzyme Mix	1
RNA	1 to 3,5
Nuclease-free water	15µl - RNA µl

For the first cDNA synthesis step, the reaction was performed at 42 °C for 1h. The Reverse Transcriptase enzyme was inactivated at 80 °C for 5 min. Finally, for 500 ng of PCR-solution, the sample was diluted with 180 µl PCR-water to reach the final volume of 200 µl, and stored at –20 °C.

4.3.3 qPCR procedure

Quantitative real-time PCR (qRT-PCR) was performed by using a qPCR Master Mix in triplicate. The qPCR analysis and sample preparation were performed in 384-multiwell plates. 2 µl of cDNA of each set of samples was pipetted in three wells. Then, to the cDNA, 8 µl of Master Mix was added, containing the gene of interest. Then, for the analysis of the next gene, the same procedure was performed by changing the primer sequence inside the new Master Mix created. 16 different genes were in total analyzed. The Master Mix composition with volumes is shown in the following table 4.5. Primers used were listed in the material section, table 3.1.

Table 4.5 - qPCR Master Mix reaction

Ingredients	**Volume (for 1 reaction, µl)**
SYBR Green	5
Primer fw	0.3
Primer rv	0.3
ddH20	2.4

The qPCR reaction was then carried out using Quant studioTM 6 Flex Real-time PCR System. Ct values for each tested gene were normalized with the Ct values of house-keeping gene Eef1α1, and calculated by ΔΔCt method.

4.4 HPLC taurine sample processing

A range of 9-12 mg tissue was weighed in a precellys tube containing 5 ceramic beads. After MeOH absolute (−20 °C) nine times of the volume was added, the samples were homogenized in the Precellys Tissue Homogenizer (Bertin Instruments, Montigny-le-Bretonneux, France) twice for 15 s at 5.000 x 2 rpm until tissue disruption. After being shaken in a cool room for 10 min and then vortexed the samples were centrifuged for 10 min 18000 x g at 4 °C. After transferring the supernatant into a new tube, samples were centrifuged again for 10 min 18000 x g at 4 °C to remove the remaining debris. Finally, supernatants were transferred into HPLC vials for measurement. All the steps were performed on ice to avoid denaturation of the samples.

4.4.1 Preparation of the standards

The Solvent A was prepared by adding 0.1% formic acid to ROTISOLV HPLC gradient grade water, while in Solvent B + 0.1% formic acid was added to ROTISOLV HPLC gradient grade acetonitrile. HPLC method was configured for a measurement duration of 10 min for each sample, with washing steps every 5 samples.

To establish the amount of taurine in the samples, a series of standard curves for taurine, GSH, and taurine/GSH were prepared. 2 mg of taurine and GSH were dissolved in 500 µl of HPLC grade water and 500 µl of MeOH to create a standard stock, and then vortexed. Next, stock solutions were diluted by adding 900 µl MeOH (STD A), followed by further dilution in series generating aliquots at decreasing amounts of taurine or GSH concentration (STD 1 to 10). At each dilution step, the aliquot was vortexed.

For the generation of the G/T standard curve, STD 1 was generated by mixing 100 µl of both taurine stock solution and GSH stock solution (200 µl final total volume), diluted with 800 µl of MeOH. Next, a dilution in series was performed again to generate aliquots with known decreasing concentrations.

4.5 Statistical Analysis

For the HPLC measurements, Shimadzu software generates peaks and the corresponding calculated Area under the Curve (AUC) for each detected m/z. To accurately identify the peaks, the anticipated retention times for each conjugate are considered. The concentration of taurine, GSH, and taurine-GSH in the samples was determined based on the standard curve. Statistical analysis was performed by ANOVA single factor. Differences between the groups were considered statistically significant when $p<0.05$.

5. Results

5.1 Histology

5.1.1 The effect of CR regiment and low-taurine diet on eWAT and BAT

Since the aim of this study was to examine the CR role on adipose tissue loss and, particularly, its effect on WAT browning, histological sections of both eWAT and BAT samples were prepared as previously described (see 4.2) and stained with hematoxylin and eosin method.

Histological sections of both *ad lib* control and CR mice displayed as expected large lipid droplets of adipocytes in eWAT with little cytoplasm around and a de-centered nucleus (Figure 5.1 A and B). Furthermore, the BAT section showed smaller brown adipocytes compared to the white ones, with a lower amount of lipid droplets. However, no additional differences were observed in BAT sections after CR treatment compared to the BAT *ad libitum* control (Figure 5.2 A and B)

Next, we combined the CR regime with low-taurine diet; as a control, we used *ad libitum* low-taurine diet mice. eWAT sections of both *ad libitum* LTD and CR in combination with LTD show large white adipocytes (Figure 5.1 C and D). BAT sections showed again as expected smaller brown adipocytes compared to the white ones, with a lower amount of lipid droplets (Figure 5.2 C and D).

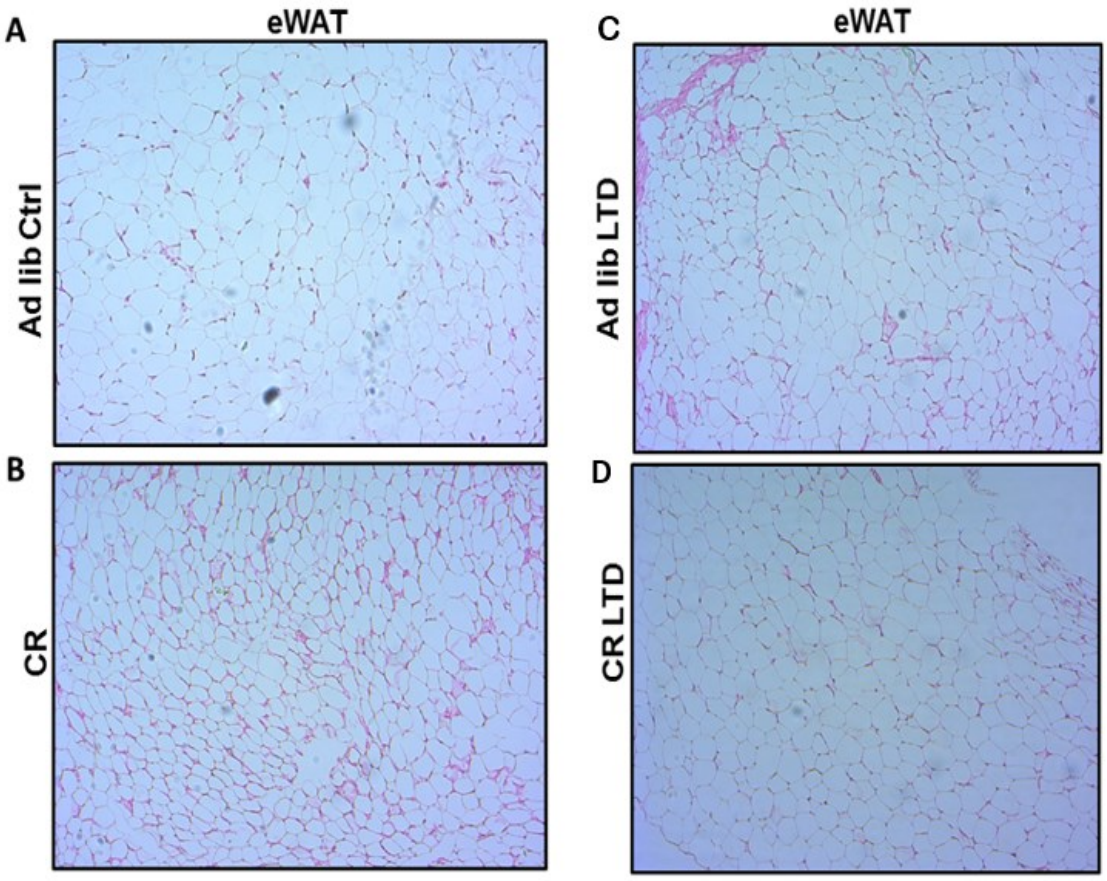

Figure 5.1 –The effects of calorie restriction and low-taurine diet with and without CR regiment on eWAT: (A) Mice control *ad libitum* fed 10x magnification (B) Calorie restriction nutritional approach 10x magnification. (C) Mice control *ad libitum* fed with low-taurine nutritional approach 10x magnification. (D) Calorie restriction with low-taurine diet 10x magnification. Figures are representative of eight different sections. Tissue sections were 4 µM. *Ad lib* Ctrl = *Ad libitum* control; CR = Calorie restriction; LTD = low-taurine diet; eWAT = epididymal white adipose tissue

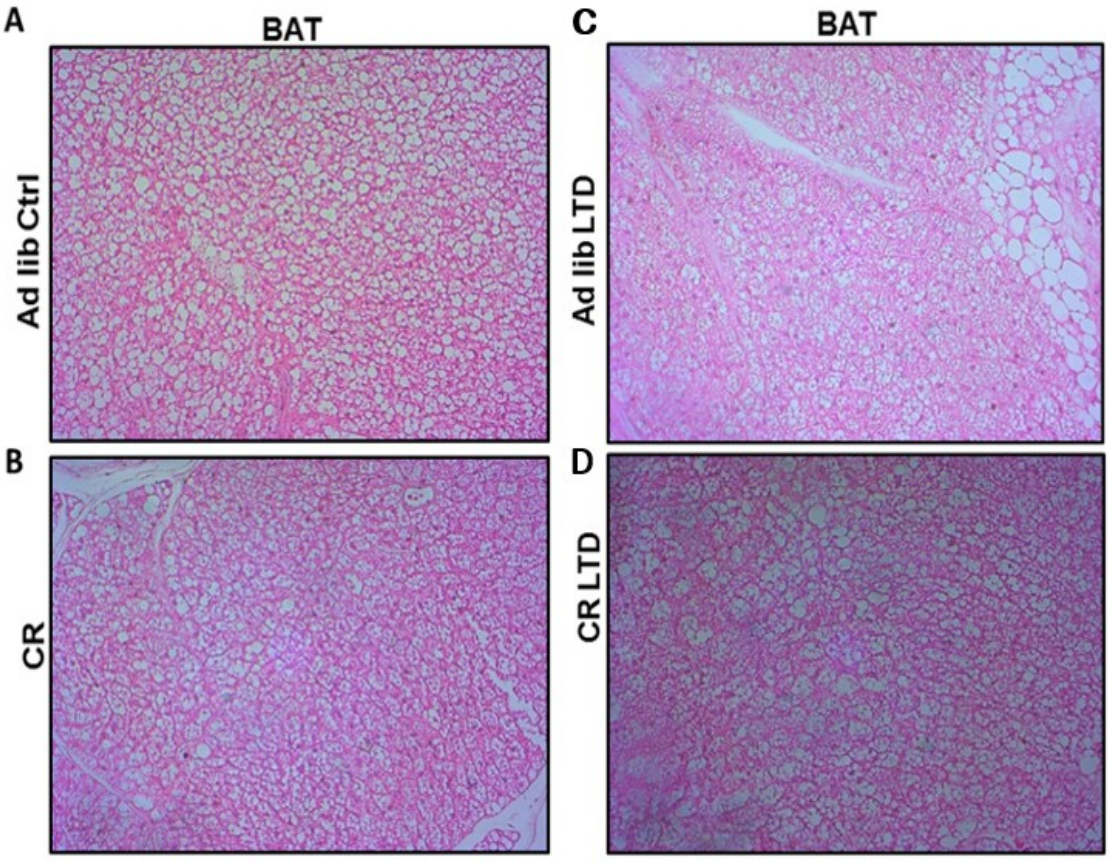

Figure 5.2 – The effects of calorie restriction and low-taurine diet with and without CR regiment on BAT: (A) Mice control *ad libitum* fed 20x magnification. (B) Calorie restriction nutritional approach 20x magnification. (C) Mice control *ad libitum* fed with low-taurine nutritional approach 20x magnification. (D) Calorie restriction with low-taurine diet 20x magnification. Figures are representative of eight different sections. Tissue sections were 4 µM. *Ad libitum* Ctrl = *Ad libitum* control; CR = Calorie restriction; LTD = low-taurine diet; BAT = brown adipose tissue.

Despite no significant differences being observed under the microscope on the LTD effect on eWAT tissue compared to the *ad lib* control (Figure 5.1), the number of the adipocytes counted per area in eWAT *ad lib* LTD samples decreased compared to the *ad lib* control, suggesting the presence of smaller adipocytes. Cell area average number significantly decreased after CR treatment compared to the *ad libitum* control (Figure 5.3) in eWAT samples. Cell area average number is also decreased in BAT samples under CR regiment; in this case, we also observed a decreased cell area under CR combined with LTD (Figure 5.3).

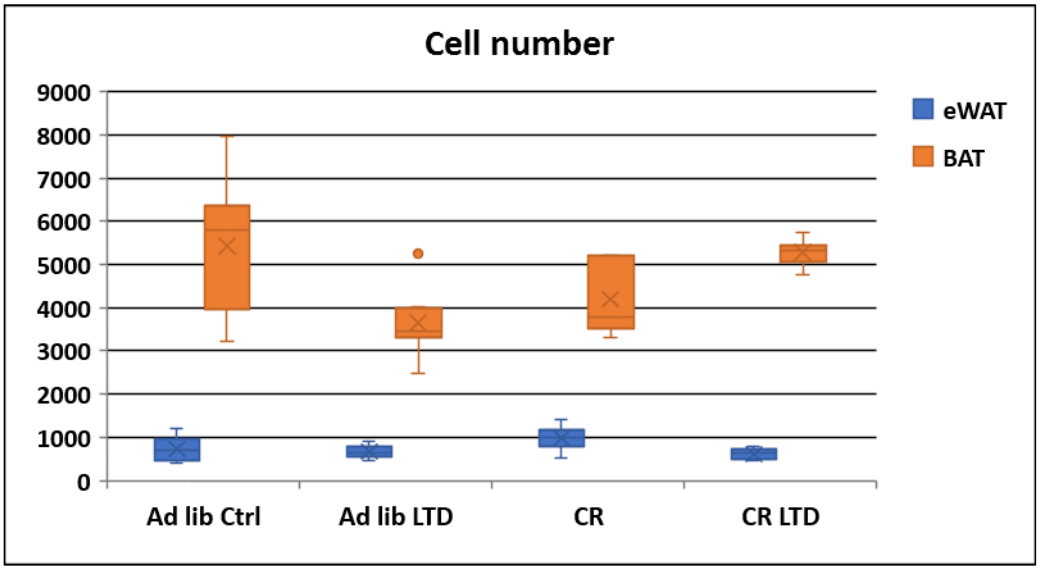

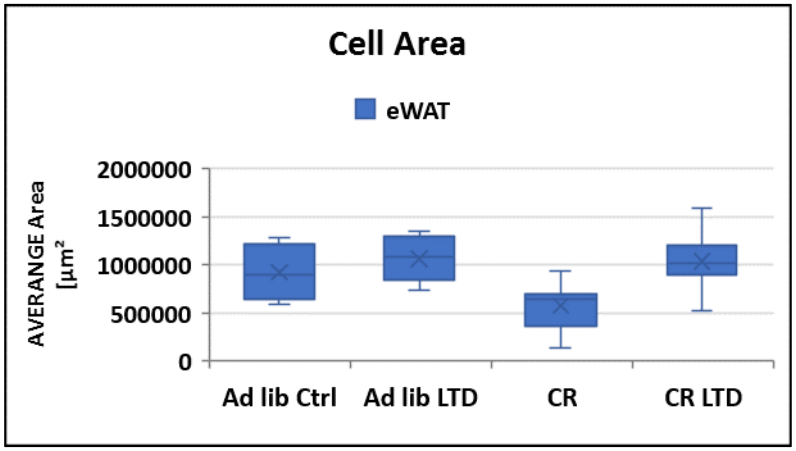

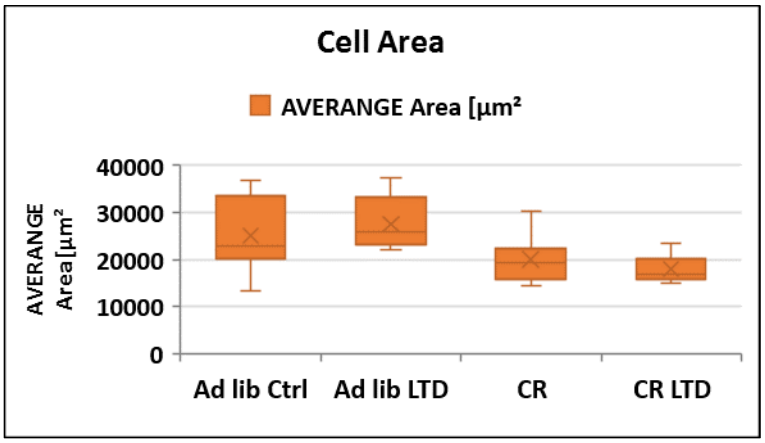

Figure 5.3 – Comparison of adipocyte number and cell area under LTD treatment in combination or not with CR in eWAT (blue bars) and BAT (orange bars) mice tissue. Numbers are an average from 8 independent mice comprising the same group of dietary intervention.

5.1.2 Cage bedding in combination with CR regiment effect on eWAT and BAT

To better understand whether cage bedding might have an impact on adipose loss, a CR has been proposed in combination with cage bedding or not. Thus, two groups of mice have been treated under CR, with or without bedding, and compared to the *ad-lib* control, with or without bedding as well.

Histological sections of *ad lib* control with bedding displayed large lipid droplets in eWAT adipocytes (Figure 5.4 A). Surprisingly, the CR mice with bedding showed smaller adipocytes surrounded by cytoplasm, and a higher tissue vascularization, resembling brown adipocytes morphology (Figure 5.4 and 5.5 B)

Next, following the same approach we analyzed the effect of no cage bedding under CR or not *(ad libitum* no bedding was used as mice control group). Again, histological analysis demonstrated differences in white adipocyte morphology and size in CR no bedding sample compared to *ad libitum* no bedding control (Figure 5.4 C and D). CR mice without bedding tissue sections resemble brown adipocyte morphology (Figure 5.4 and 5.5 D).

BAT histological sections revealed increased brown adipocyte size in *ad libitum* no bedding control compared to the CR no bedding mice group, suggesting the presence of more amount of lipid droplets (Figure 5.5 C and D).

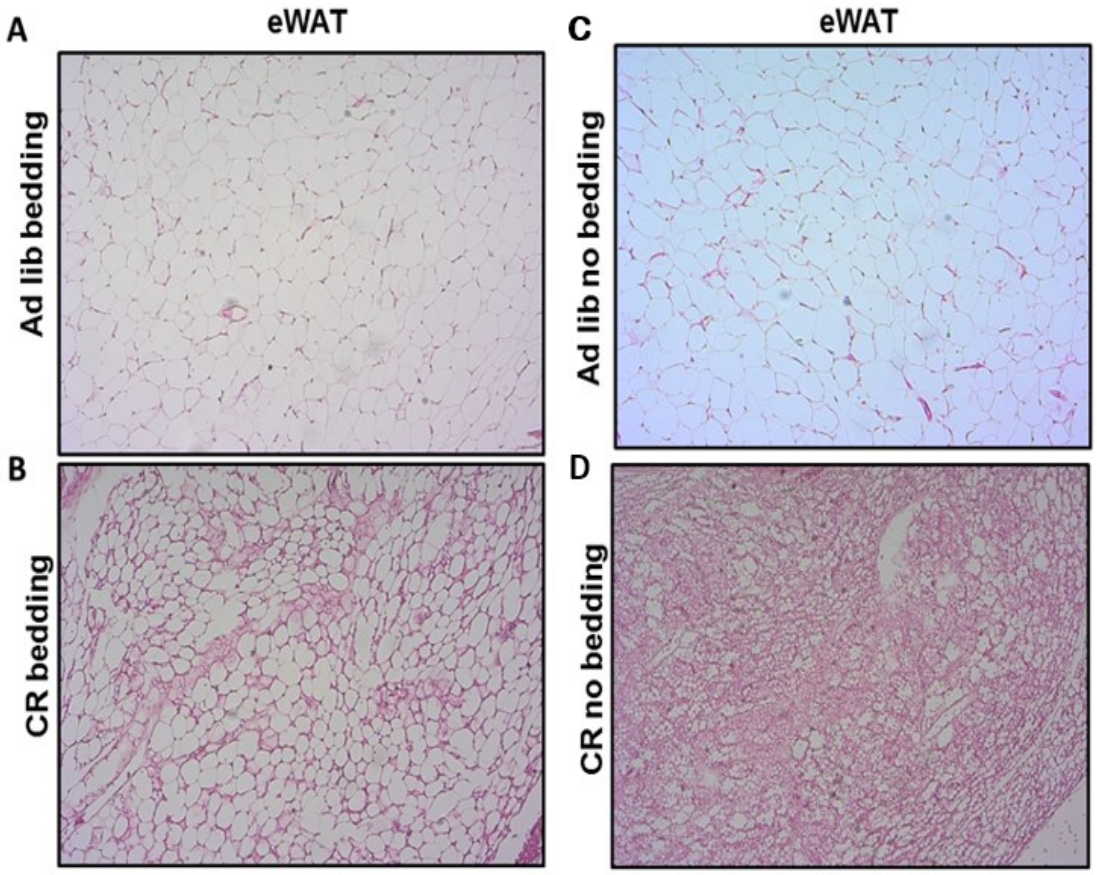

Figure 5.4 – CR nutritional approach with and without bedding effect on eWAT (A) Mice control *ad libitum* fed with bedding, 10x magnification. (B) Calorie restriction nutritional approach with bedding 10x magnification. eWAT CR bedding sample displayed smaller white adipocytes surrounded by cytoplasm resembling brown adipocytes (Figure 5.5 B) (C) Mice control *ad libitum* fed without bedding, 10x magnification. (D) Calorie restriction nutritional approach without bedding; 10x magnification; adipocytes resemble the morphological composition of BAT 20x magnification observed in Figure 5.5. The absence of bedding in the cage further enhances the white adipose tissue morphological similarities to the BAT ones. Figures are representative of eight different sections.Tissue sections were 4 µM. *Ad lib* = *Ad libitum*; CR = Calorie restriction; eWAT = epididymal white adipose tissue; BAT = brown adipose tissue

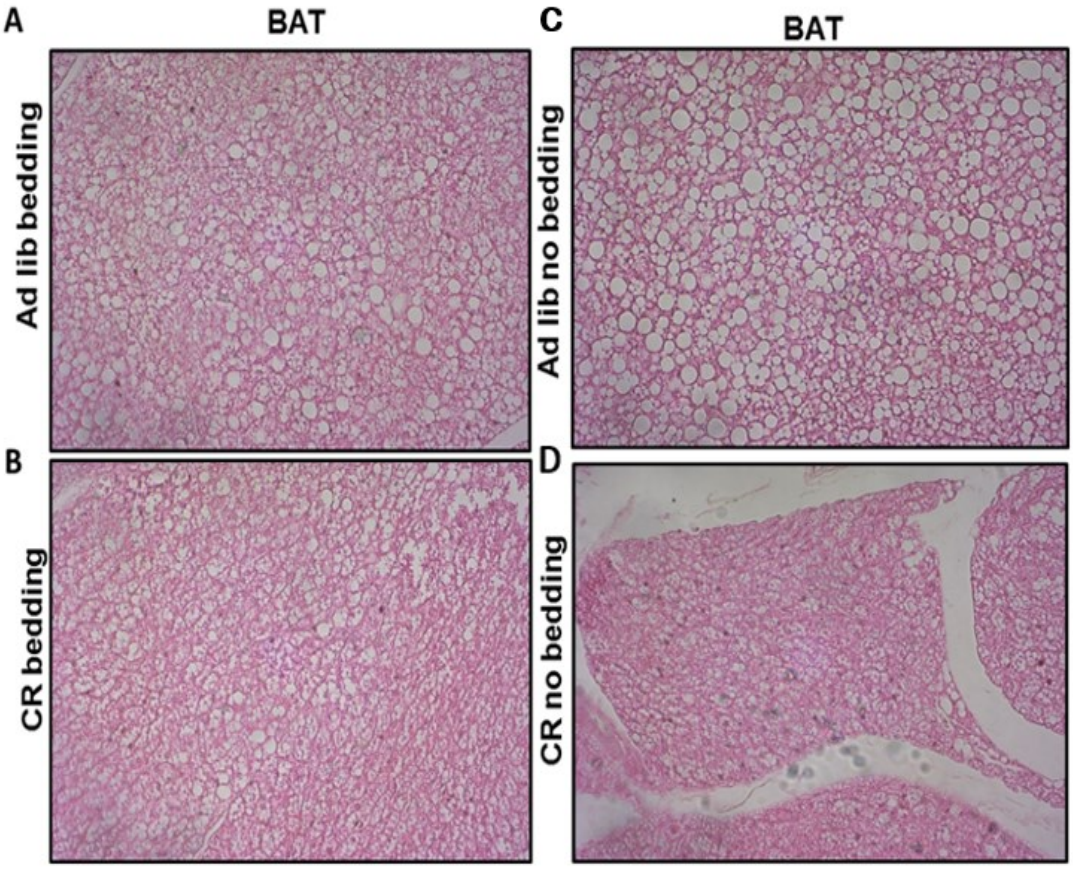

Figure 5.5 – CR nutritional approach with and without bedding effect on BAT (A) Mice control *ad libitum* fed with bedding, 20x magnification. (B) Calorie restriction nutritional approach with bedding 20x magnification. (C) Mice control *ad libitum* fed without bedding, 20x magnification. Brown adipocytes showed an increased lipid droplet compared to the *Ad libitum* bedding one (A); (D) Calorie restriction nutritional approach without bedding; 20x magnification. Figures are representative of eight different sections. Tissue sections were 4 μM. *Ad lib = Ad libitum*; CR = Calorie restriction; BAT = brown adipose tissue.

Further data evaluation demonstrated a higher number of adipocytes in CR with bedding samples compared to the *ad libitum* with bedding control per area calculated, suggesting a smaller adipocyte size in the tissue (Figure 5.6). However, when we compared the number of white adipocytes counted per area in CR mice with or without bedding, we observed an increased number of white adipocytes when the mice were placed in a cage without bedding, suggesting that the additional bedding removal to the cage increases the effects of CR diet and might improve the browning process (Figure 5.6). Moreover, the brown adipocytes counted per area in *ad libitum* no bedding control mice significantly decreased compared to the CR bedding mice, supporting the picture observed (Figure 5.6).

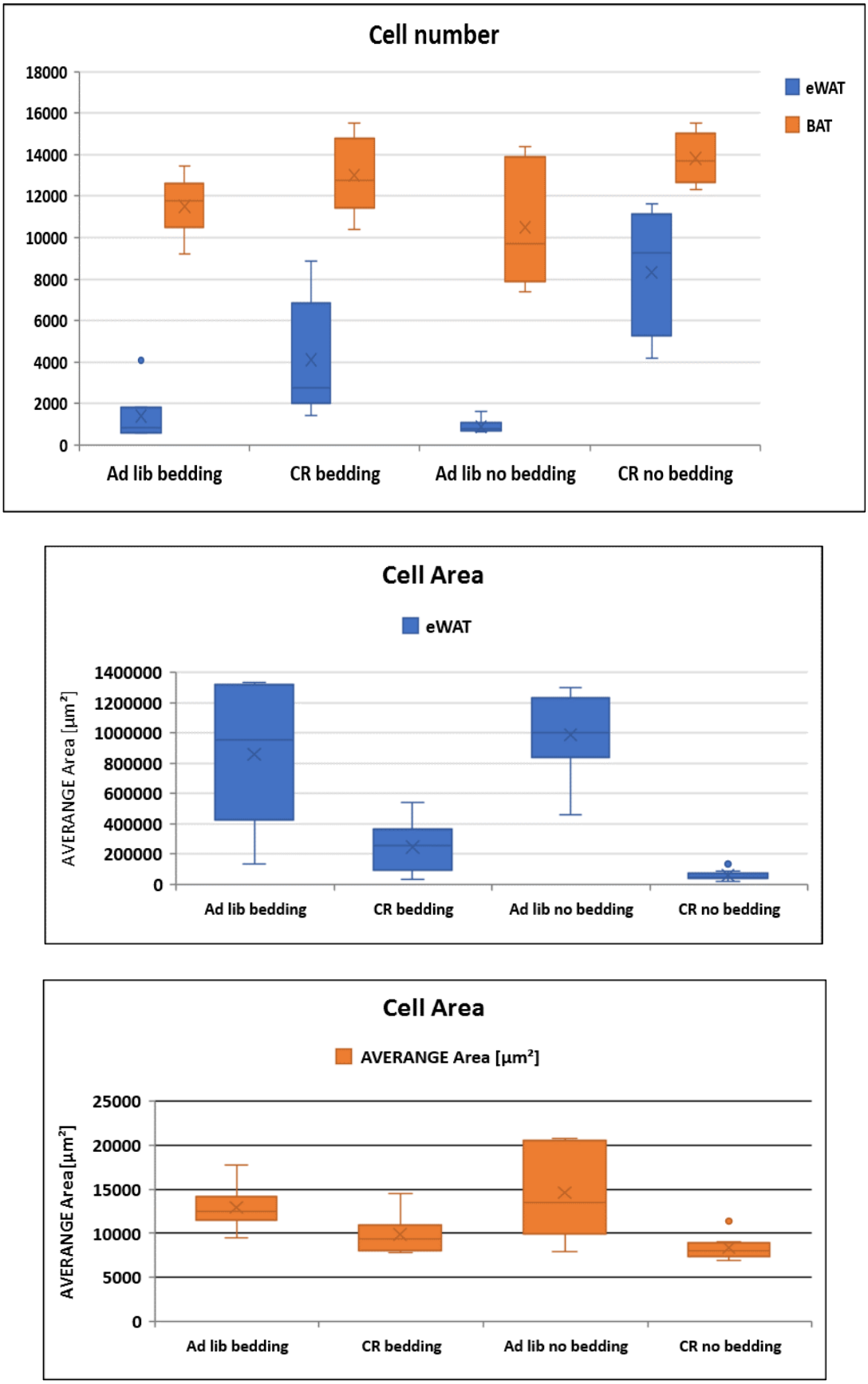

Figure 5.6 – Comparison of adipocyte number and cell area in eWAT (blue bars) and BAT (orange bars) in mice under CR nutrient intervention with or without cage bedding. Numbers are an average from 8 independent mice comprising the same group of dietary intervention.

In conclusion, these preliminary data suggest that CR regiment might affect the white browning process in epididymal white tissue, which is further enhanced by the removal of cage bedding. However, additional experiments (such as qPCR analysis) are requested to support the presented data.

5.1.3 Different fat and carbohydrates composition in CR diet analysis on eWAT

After investigating the effects of CR on adipose tissue, we wanted to observe whether a specific macronutrient caloric restriction might impact white adipose tissue morphology, as well as adipocyte size and number. Since it has been described in the previous chapter (see 1.1) that either fat or carbohydrates lower calorie intake present similar phenotypes as calorie restriction regimen, we divided mice into five groups following different nutritional approaches based on the daily intake reduction of these two macronutrients (already described in 4.1; table 4.2 and 4.3). Thus, histology tissue analysis under a microscope revealed no significant differences in the adipocyte morphology between the control and the low-fat or low-carb diets (Figure 5.7).

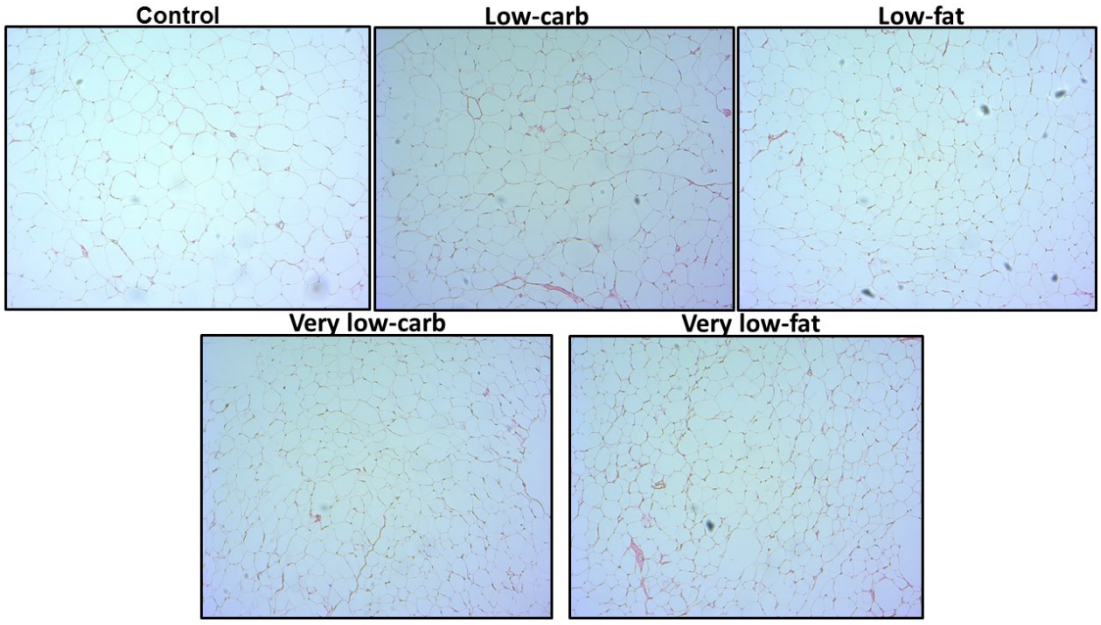

Figure 5.7 – Fat and carbohydrates reduction intake diet on white adipose tissue. All the eWAT sections are 10x magnification. Control, low-carb, and very low-fat figures are representative of eight different sections; low-fat figure is representative of seven different sections; the very low-carb figure is representative of five different sections. Tissue sections were 4 µM. Carb = carbohydrates

Furthermore, we observed a decrease in cell number after low-carb and very-low-fat diets compared with the control, while no significative differences have been identified after low-fat and very-low carbs nutritional approach in eWAT mice histological samples (Figure 5.8).

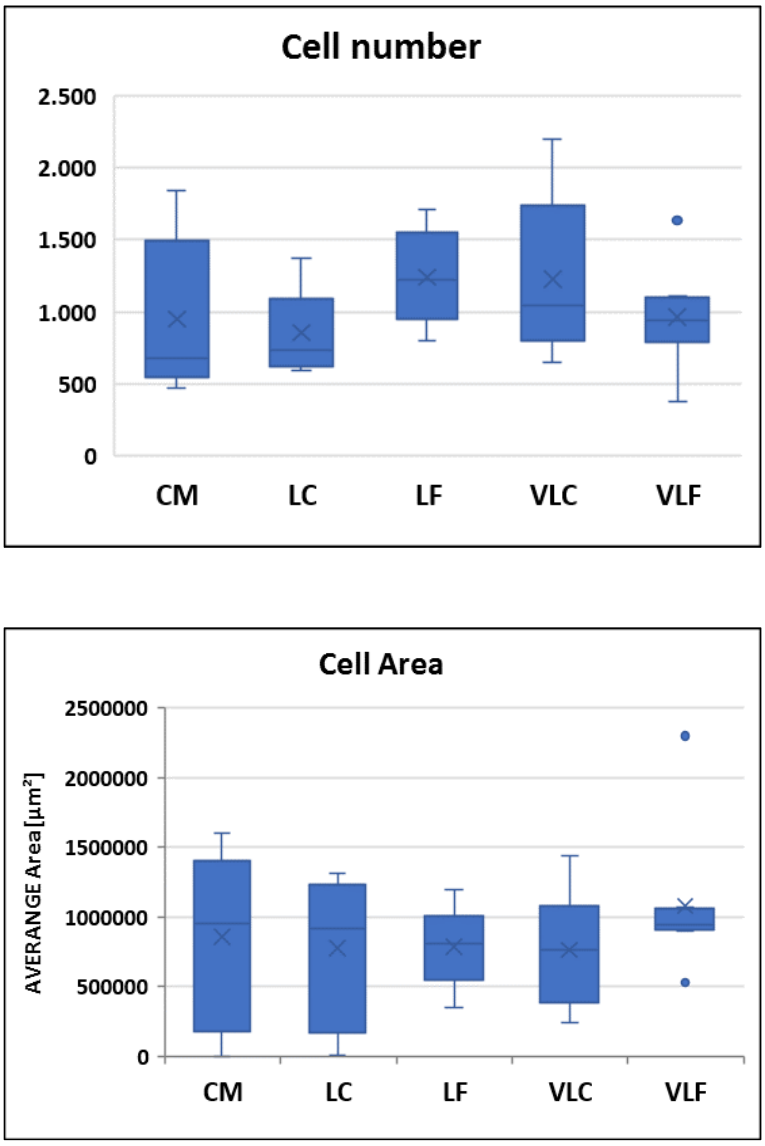

Figure 5.8 – Evaluation of the number and average cell area of eWAT histological analysis after low/very low fat and carbohydrates diet. Numbers are an average from different independent mice tissue sections comprising the same group of dietary intervention; Control, low-carb, and very low-fat values are an average of eight sections; low-fat values are an average of seven sections; very low-carb values are an average of five sections. CM= custom made control, LC=low-carbohydrates, LF= low-fat, VLC= very low-carbohydrates, VLF= very low-fat.

5.2 qPCR

5.2.1 Gene-expression analysis in eWAT and BAT after CR regiment and low-taurine diet

After histological tissue morphology analysis (see 5.1.1), to further investigate whether CR regiment in combination with low-taurine diet might affect the white adipose tissue browning process, the gene-expression analysis was performed on the same group of mice. Some significant genes involved in the browning process were then analyzed, as well as genes involved in taurine metabolism. RNA precipitation and cDNA synthesis were already described before (see 4.3.2). Primer's sequence list of the analyzed genes is listed in Table 3.1. Data are shown as an average of eight independent cDNA samples comprising the eight mice per dietary group treatment. Calculations have been performed following the ddCT fold change method, and the y-axis shows the fold change values. The standard deviation has been calculated from the average of each gene with Excel. The same set of genes was analyzed in both eWAT and BAT samples.

Gene expression analysis revealed that *ad-lib* LDT regiment alone significantly increases the mRNA expression in the majority of the genes analyzed in eWAT, such as UCP1 (Fold Change (FC) = 1.74) and UCP2 (FC=1.56), ACOT4 (FC=1.76), and ACSL3 (FC=2.07), which was the most upregulated gene, compared to the *ad libitum* control (Figure 5.9, blue bar = control; orange bar = LDT). However, the CR diet led to a decrease in gene expression of the analyzed compared to the *ad libitum* control (Figure 5.9, grey and blue bars, respectively), suggesting that reduction of calorie intake alone interferes with the gene expression. Interestingly, CR combined with LTD diet led to an upregulation of CDO (FC=2.13) compared to the *ad-lib* LTD diet, were CDO FC=1.57. Finally, CR diet decreases PPARγ expression (FC=0.77) compared to the *ad libitum* control (FC=1.10), but LTD combination with CR allows the gene expression to reach a comparable level of expression (FC=1.28) as *ad libitum* LTD (FC=1.16) sample.

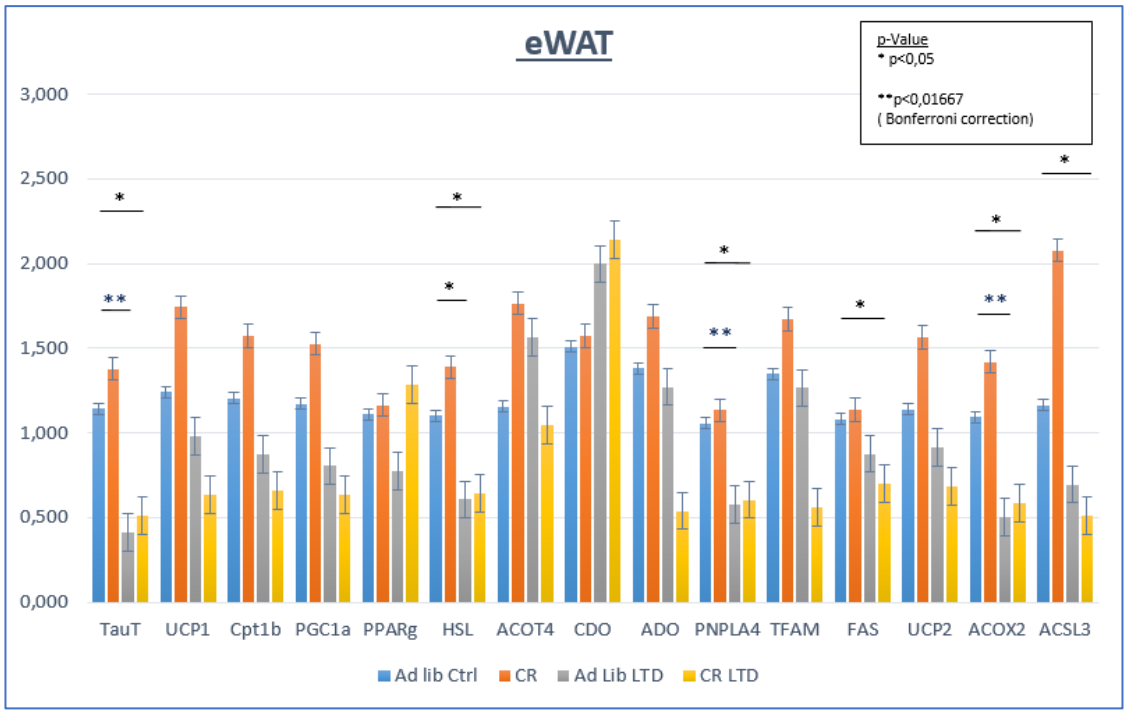

Figure 5.9 - Gene expression analysis in eWAT after CR in combination or not with LTD diet.

The same gene expression analysis was performed also in the BAT set of samples. In brown adipose tissue, the majority of the analyzed gene expression decreased under *ad lib* LTD treatment compared to the *ad libitum* control (Figure 5.10 orange and blue bars, respectively). UCP1 (FC=1.75) and PPARγ (FC=2.48) are the only upregulated genes found in BAT samples under *ad lib* LTD treatment compared to the *ad libitum* control. In BAT samples, low-taurine diet in combination with CR, highly increases the gene expression of ACOT4 (FC=2.67), ADO (FC=3.21), TFAM (FC=2.97), ACOX2 (FC=2.45), UPC2 (FC=1.77), and ACSL3 (FC=2.53), compared to both *ad libitum* fed and CR mice (Figure 5.10, yellow, blue and gray bars, respectively).

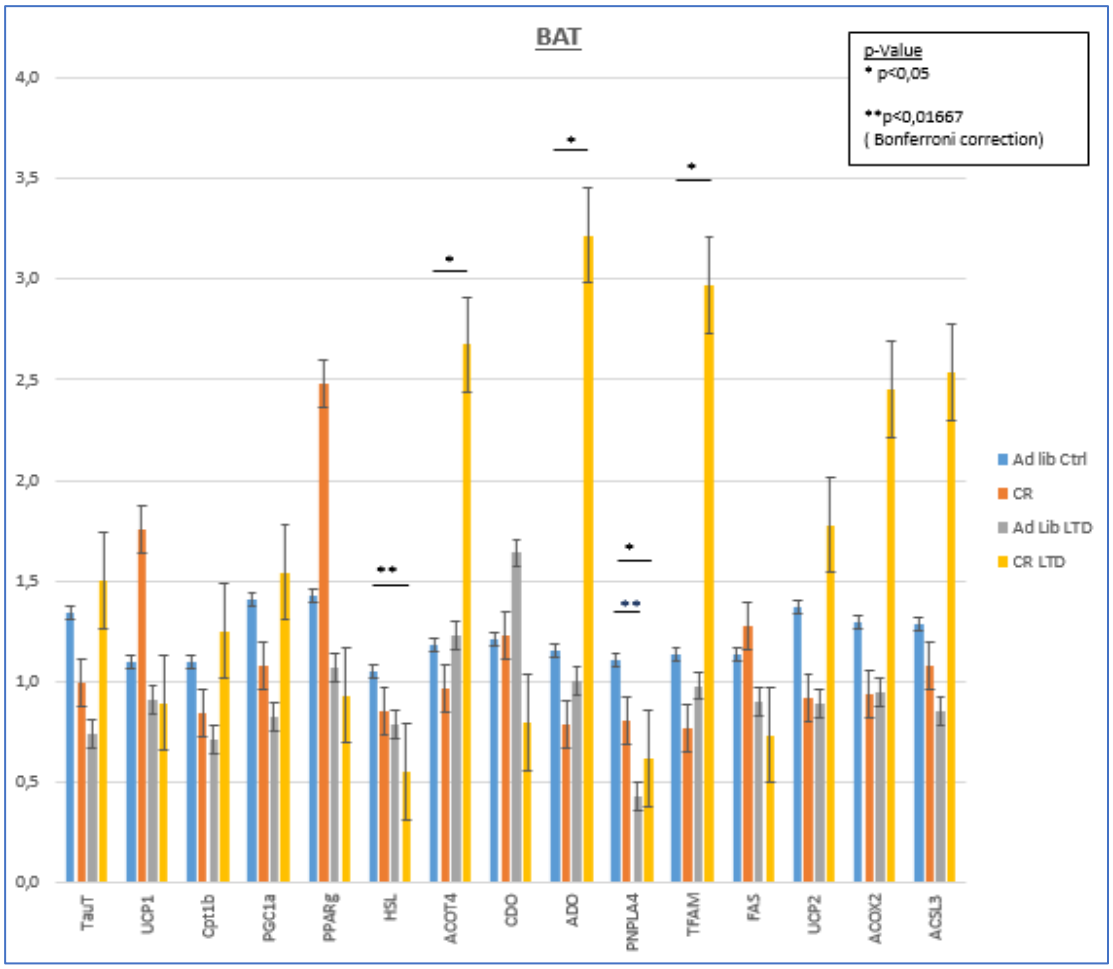

Figure 5.10 - Gene expression analysis in BAT after CR in combination or not with LTD diet.

5.2.2 Gene-expression analysis in eWAT and BAT CR regiment with cage bedding

Histological tissue analysis (see 5.1.2) revealed that mice under CR regiment without cage bedding showed some similarities between eWAT and BAT, suggesting the eWAT browning process. Thus, gene-expression analysis was performed to better understand whether, in the same conditions, browning of white tissue occurs.

In the eWAT samples, genes were found significantly up-regulated under CR conditions independently of bedding (orange bars) or without bedding (yellow bars), such as TauT (FC=2.10 and FC=1.88, respectively), CDO (FC=1.63 and FC=1.75, respectively), and PGC1α (FC=0.92 and FC=1.46, respectively), compared to the *ad libitum* control. Among the upregulated genes, ACOT4 is also found to increase in expression under CR (FC=3.48); however, CR combined with no-bedding cage enhances this increase (FC=5.17). On the other hand, another set of genes was found significantly downregulated under both

CR and CR without bedding treatment, like ADO (FC=0.41 and FC=0.40) or UCP2 (FC=0.75 and FC=0.98), compared to the *ad libitum* control. No significant differences were found where the mice were normally fed but without cage bedding compared to the *ad libitum* control (Figure 5.11).

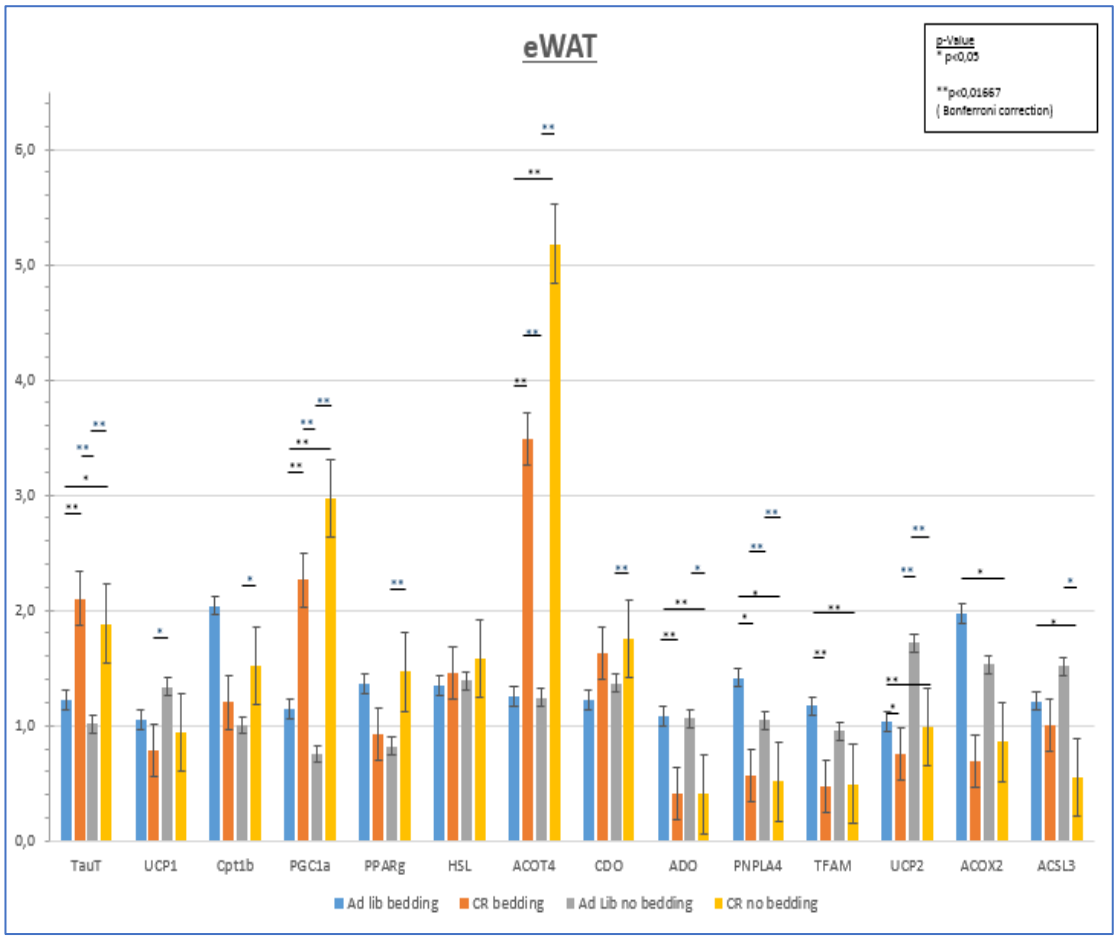

Figure 5.11 - Gene expression analysis in eWAT after CR treatment with or without cage bedding.

Under the same conditions, we performed gene-expression analysis on BAT samples. The same set of genes found upregulated under both CR and CR no bedding conditions in eWAT samples were found increased only under CR no bedding condition (yellow bar): TauT (FC=3.68), and PGC-1α (FC=2.52). ACOT4 is highly upregulated under CR treatment (FC=5.26, orange bar), but the combination with no-bedding cage decreases its expression (FC=3.59, yellow bar). Among the most upregulated genes under CR treatment in BAT, we found significantly increased expression of UCP1 (FC=2.05) and CDO (FC=3.14) compared to the *ad libitum* control. Interestingly, the well-established browning marker UCP1 is found downregulated under CR-no

bedding condition (FC=0.60, yellow bar) compared to both *ad libitum* (blue bar) and *ad libitum* no bedding control (grey). CR no bedding condition led to the increased gene expression of ACOX2 (FC=3.50) and ACSL3 (FC=4.54), found to be downregulated under the same condition in eWAT samples (Figure 5.11).

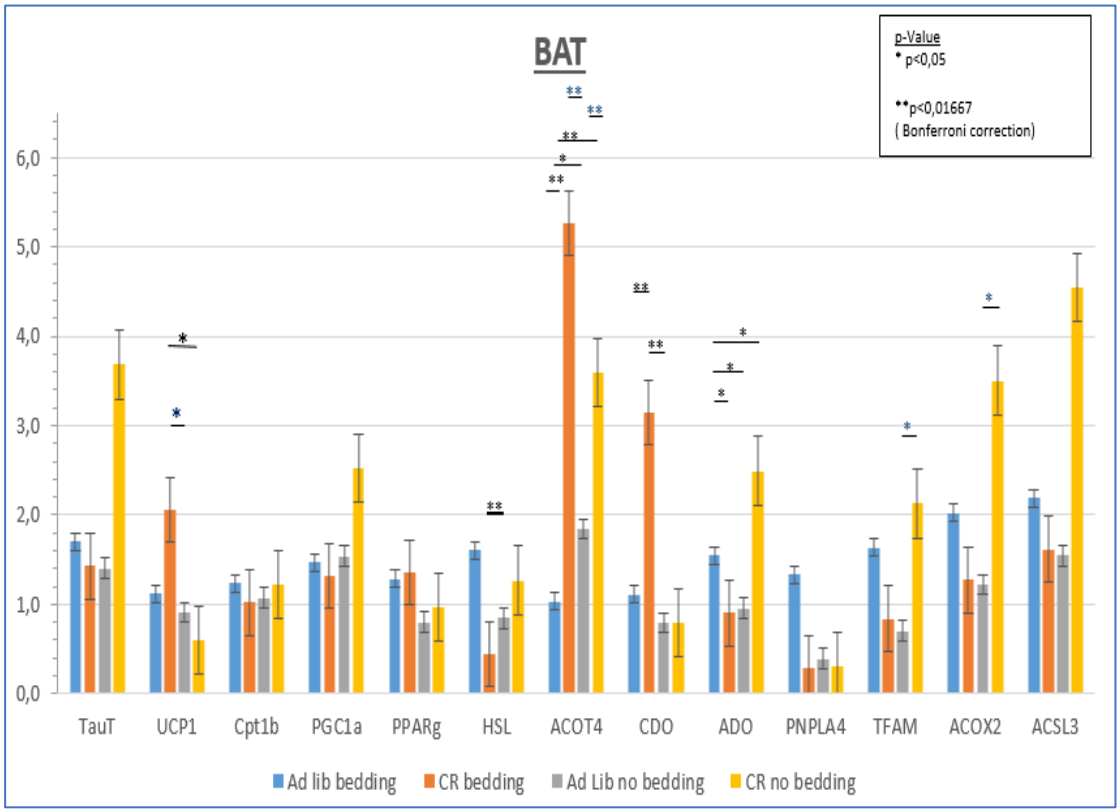

Figure 5.12 - Gene expression analysis in BAT after CR treatment with or without cage bedding.

5.2.3 Gene-expression analysis in BAT

Since the qPCR analysis expression revealed a significant dysregulation for some selected genes after low-taurine diet combined with or without CR regiment in brown adipose tissue (see 5.2.1, Figure 5.6), we wondered whether we might observe significant changes after the addition to the mice CR diet with taurine.

Taurine supplementation in the *ad-lib* mice group decreases the expression level of TauT (FC=0.69) compared to the *ad libitum* control (Figure 5.10, orange and blue bars, respectively). Additional genes found downregulated after taurine supplementation were ADO (FC=0.65), TFAM (FC=1.08), and ACSL3 (FC=0.84). However, both PPARγ (FC=1.63) and CDO (FC=1.75) were found

upregulated compared to the *ad libitum* control (orange and blue bars, respectively), suggesting a taurine involvement in their gene-regulation.

CR regiment alone increases the gene expression of HSL (FC=1.84, grey bar) compared to the other samples, but the taurine supplementation diet restores HSL expression (yellow bar) as the *ad libitum* control (blue bar). Moreover, CR regiment decreases UCP1 expression levels (FC=0.67, grey bar), which is further enhanced when CR is combined with taurine supplementation (FC=0.52, yellow bar). Finally, CR combined with taurine (yellow bars) significantly upregulates TFAM (FC=2.01) and ACOX2 (FC=2.0), which is also found to increase with CR diet alone (FC=1.95, orange bar) (Figure 5.13).

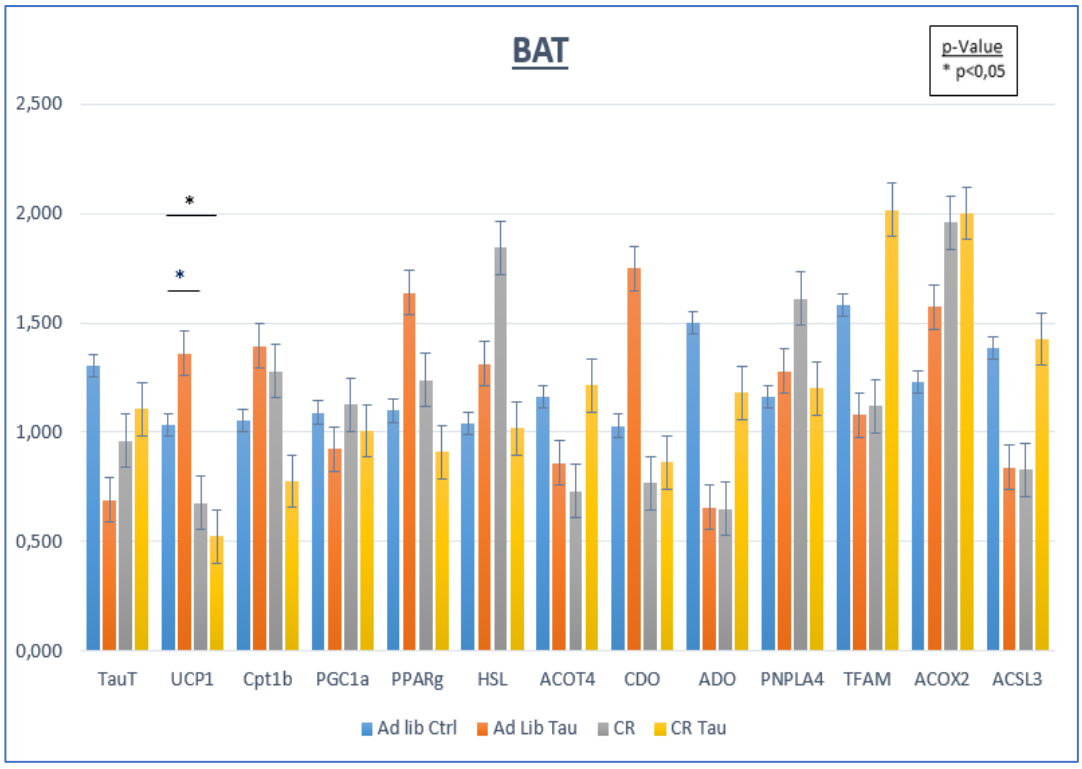

Figure 5.13 - Gene expression analysis in BAT after CR treatment with or without taurine supplementation.

5.3 MS/HPLC results

5.3.1 HPLC eWAT and BAT

MS/HPLC was used to measure taurine and GSH composition in both white and brown adipose tissue under CR combined with or without low-taurine diet. As control was used *ad libitum* normally fed mice group (see also 4.1).

MS/HPLC analysis shows increased taurine levels in CR samples compared to *ad libitum* control (Figure 5.14) in white adipose tissue. When mice were under an *ad libidum* LTD regimen taurine levels were slightly decreased compared to the *ad libitum* control.

Moreover, GSH levels increase in the CR diet as well, while no differences have been observed among the other conditions in eWAT samples compared to the *ad lib* control (Figure 5.14).

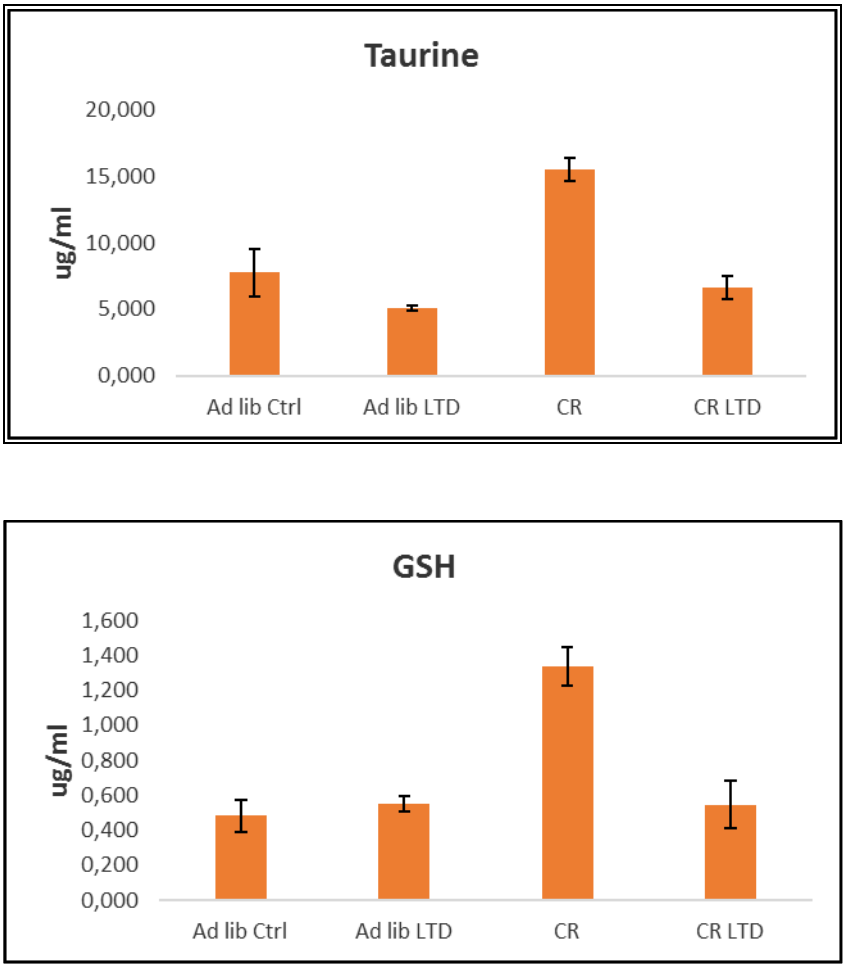

Figure 5.14 – Taurine and GSH amounts [ug/ml] in eWAT tissue. Comparison between *ad libitum* normally fed mice group (*ad lib* Ctrl), calorie restriction mice treatment (CR), *ad libitum* with low-taurine diet mice group (*ad lib* Ctrl LTD), and calorie restriction mice treatment combined with low-taurine diet (CR LTD).

On the other hand, MS/HPLC measurements performed in BAT samples revealed a weak increase of taurine levels in CR samples (Figure 5.15), but no significant changes have been found among the other conditions. Finally, GSH levels increased in CR samples, while LTD combined with CR regiment slightly decreased GSH amount in BAT, leading to a closer value as the *ad libitum* control.

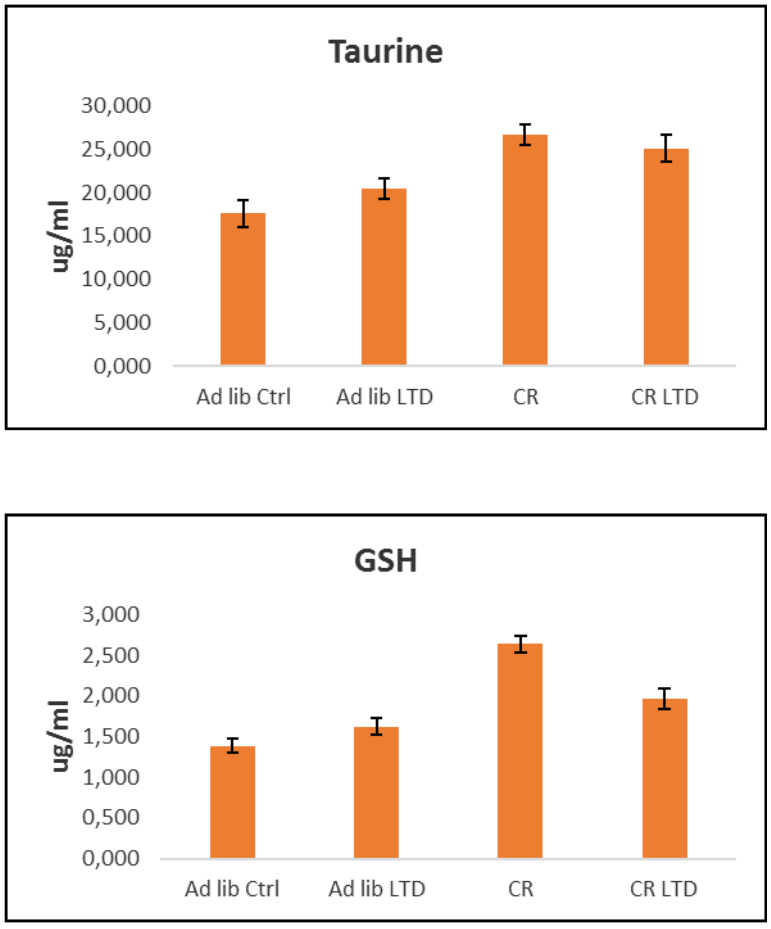

Figure 5.15 - Taurine and GSH amounts [ug/ml] in BAT tissue. Comparison between *ad libitum* normally fed mice group (*ad lib* Ctrl), calorie restriction mice treatment (CR), *ad libitum* with low-taurine diet mice group (*ad lib* Ctrl LTD), and calorie restriction mice treatment combined with low-taurine diet (CR LTD).

6. Discussion

This study aimed to examine the CR's role in adipose tissue loss. Moreover, it has been described in the introduction chapter that taurine influences weight loss and energy production (see 1.1.). Specifically, under LTD taurine, cysteine, and methionine are not included, which impedes mice's ability to produce taurine endogenously. Furthermore, taurine has been proposed as a potential supplement to replicate the benefits of CR [5], and it is known that taurine supplementation influences lipid metabolism [31]. According to our data, both taurine dietary and endogenously produced contribute to this outcome.

Previously, we demonstrated in mice that CR promotes both hepatic taurine and bile acid synthesis and conjugation, thus released into the GI tracts. Then, bile acids are modified by microbial BSH in the intestine, leading to their release as deconjugated bile acid and free taurine. Thus, free taurine is re-uptaken into the bloodstream by its transporter *TauT*, whose expression is increased in the CR intestinal mucosa. Moreover, the increased taurine amount in CR mice intestines affects CR-related adipose tissue loss [5, 32-35].
Based on these findings, after being released from bile acid in the intestine, free taurine is preferentially transported to WAT tissue compared to other tissues. To further investigate this process, we labeled and dosed taurine in WAT. By testing its abundance, our data suggest that taurine increased levels in WAT originate mostly from the intestinal pool. To support these findings and the enhanced taurine uptake, gene expression assay revealed increased gene followed by protein synthesis of TauT in CR mice eWAT. Since we also observed an elevated expression of CDO gene in eWAT, we speculate that taurine biosynthesis may be enhanced in CR adipocytes.

Our previously published data suggest that CR results in total body weight loss compared to IF and FMD mice [8, 23]. The observed outcome is probably due to the more stringent dietary restrictions CR compared to IF and FMD dietary regimes. Under CR, mice experience intense hunger, and consequently, they consume more cage bedding, which promotes BSH activity, resulting in enhanced taurine levels and, consequently, in its conjugates in the intestine. Our findings suggest that eWAT taurine amounts are directly influenced by changes

in the taurine concentration in the intestine. In addition, cage bedding and soluble fiber consumption promote bile acid deconjugation, resulting thus to increased taurine conjugate levels rather than insoluble fiber. The same occurs in the eWAT taurine levels presented in this study, further supporting the direct correlation existing between the intestinal and eWAT taurine [36].

In the present study, we also measured taurine levels in CR BAT mice, which also showed an accumulation of taurine. However, taurine levels were present in smaller amounts compared to CR WAT, and the differences between the *ad libitum* control were minimal. In addition, also TauT and lipid metabolism gene-related were less affected in CR BAT compared to CR eWAT. Despite taurine supplementation affecting both BAT and WAT, we observed that LTD influenced primarily WAT but not BAT. These findings are in line with other studies in which long-term taurine supplementation reduced the expression of adipogenesis-related genes in WAT but not BAT in obese mice models [36]. Our data suggest that there is no significant impact on WAT taurine levels depending on the type of bedding. However, we observed that the absence of bedding decreased the taurine amount in WAT as we previously observed in the intestine [38]. Changes in taurine levels did not directly correlate to the body weight increase. Cage bedding is fundamental for the maintenance of warmth, which affects thermogenesis and subsequently adipose tissue [37], and we previously demonstrated that cage bedding influences CR [38]. According to that, we speculate that *ad libitum* without bedding mice compensate for thermogenesis by increasing consumption. On the other hand, CR without bedding animals dissipated more energy but without the capacity to increase food intake. This results in reduced adipose tissue. The results in this study support the outcomes of bedding-related processes previously mentioned, independent of the taurine concentration. Moreover, we showed that there is no direct correspondence between the eWAT taurine levels and eWAT weight under high-fiber diets, which affect body weight and general health. We speculate that the stronger impact of soluble versus insoluble fiber may be linked to the role of soluble fiber as a substrate for short-chain fatty acid synthesis [39-44].

Taurine supplementation increases free and conjugated taurine levels in the adipose tissue in CR animals, thus supporting weight loss and lipid metabolism in animal models and human studies [44-48]. In one study, high-fat diet-induced obese mice showed a decrease in taurine concentration in the blood, as well as a decrease in *CDO* expression. *CDO* expression was decreased specifically in adipose tissue but not in the liver [48]. Moreover, it is known that obesity represses taurine synthesis, which influences weight gain; thus, taurine supplementation might interrupt this cycle. Of notice, this study reported for the first time group an increase in taurine concentration in CR mice.

Taurine decreases fatty acid synthase (Fasn) expression and increases *Cpt1α* specifically in adipocytes. Our results demonstrate that taurine impacts the expression of several lipid metabolism-related genes, including *PGC-1α, HSL*, and *ACOX2* in eWAT. The same set of genes was regulated by CR, supporting the previously published data Wang Z. et al In their study, the authors suggest that taurine may serve as CR mimetic [49]. Finally, both CR and taurine have been shown to induce WAT browning [22]. In obesity, enlarged adipocytes secrete molecules, such as free fatty acid, TNFα, and resistin, driving chronic low-grade systemic inflammation and insulin resistance [50]. Furthermore, inflammatory processes are one of the major predisposing factors for weight [51]. Taurine is involved in multiple inflammatory mechanisms such as NFkB/COX, p38 MAPK- JNK, and MyD88 [52, 53]. Taurine supplementation downregulates pro-inflammatory mediators such as cytokines, macrophage, decreases M1 macrophages, and increases the number of M2 macrophages [54]. In conclusion, taurine supplementation might mediate and resolve inflammation, balance homeostasis, and promote the activation of metabolic processes.

In this study we also demonstrate the presence of taurine conjugates in eWAT and BAT; despite the majority of taurine conjugates is still uncharacterized, taurine-GSH (m/z 431) and taurine-chloramine (m/z 159) have been identified [5, 35]. Taurine-chloramine presents strong anti-inflammatory properties and may contribute to the beneficial anti-inflammatory impact of taurine and CR on adipose tissue [55]. Since taurine supplementation reduces food intake, another way to influence body weight is given by the regulation of the appetite.

According to our data, we measured a reduction of food intake in *ad libitum* Tau mice group compared to the control one.

Taken together, our study provides insights into taurine's role concerning fat loss. We further observed a novel communication path in which taurine acts as a messenger between the liver, gut, microbiota, and finally WAT.

7. Conclusions

The present master thesis gave the basis for future research in the weight loss field, with the aim of major investigation of the data that we have produced. The multiple treatments that we performed of CR under several additional conditions opened doors for new research insights. Gene expression analysis of low taurine treatment combined with CR regiment demonstrated the impact of this combination specifically of genes involved in mitochondria biogenesis and activity, fundamental for the proper function of adipose tissue.

CR alone already significantly dysregulates the gene expression of genes which play an important role in the browning process. This effect was enhanced and influenced by the absence of bedding in the cage, showing for the first time the possible linkage between cage bedding and weight loss tissue. Adipocyte morphological differences were visible under histological sections, with eWAT sections resembling the BAT ones. This might be a promising result for further investigation into the potential of cage bedding associated with weight loss in both healthy and obese models. This is the first report providing information that taurine restriction promotes weight loss. Our data support that under taurine-deprived diet enhances CR adipose tissue weight loss. Low-taurine diet performed in our study lacked taurine precursors since it is known that low-taurine consumption may be compensated by intake of cysteine and/or methionine-rich products.

Taken together, this work not only sets the stage for future research but also highlights the promising potential of CR modulation in a metabolic disease-related environment. Since most affected genes are related to the mitochondria activity, the molecular mechanisms and pathway regulating this organelle might be interesting for further analysis.

8. Bibliography

[1] Cena H, Calder PC. Defining a Healthy Diet: Evidence for The Role of Contemporary Dietary Patterns in Health and Disease. Nutrients. 2020 Jan 27;12(2):334. doi: 10.3390/nu12020334. PMID: 32012681; PMCID: PMC7071223.

[2] Wu Qi, Gao ZJ, Yu X, Wang P. Dietary regulation in health and disease. Signal Transduct Target Ther. 2022 Jul 23;7(1):252. doi: 10.1038/s41392-022-01104-w. PMID: 35871218; PMCID: PMC9308782.

[3] Most J, Tosti V, Redman LM, Fontana L. Calorie restriction in humans: An update. Ageing Res Rev. 2017 Oct;39:36-45. doi: 10.1016/j.arr.2016.08.005. Epub 2016 Aug 17. PMID: 27544442; PMCID: PMC5315691.

[4] Napoleão A, Fernandes L, Miranda C, Marum AP. Effects of Calorie Restriction on Health Span and Insulin Resistance: Classic Calorie Restriction Diet vs. Ketosis-Inducing Diet. Nutrients. 2021 Apr 15;13(4):1302. doi: 10.3390/nu13041302. PMID: 33920973; PMCID: PMC8071299.

[5] Gregor A, Pignitter M, Fahrngruber C, Bayer S, Somoza V, König J, Duszka K. Caloric restriction increases levels of taurine in the intestine and stimulates taurine uptake by conjugation to glutathione. J Nutr Biochem. 2021 Oct;96:108781. doi: 10.1016/j.jnutbio.2021.108781. Epub 2021 May 20. PMID: 34022385

[6] Cerqueira FM, Kowaltowski AJ. Commonly adopted caloric restriction protocols often involve malnutrition. Ageing Res Rev. 2010 Oct;9(4):424-30. doi: 10.1016/j.arr.2010.05.002. Epub 2010 May 20. PMID: 20493280.

[7] Kraus WE, Bhapkar M, Huffman KM, Pieper CF, Krupa Das S, Redman LM, Villareal DT, Rochon J, Roberts SB, Ravussin E, Holloszy JO, Fontana L; CALERIE Investigators. 2 years of calorie restriction and cardiometabolic risk (CALERIE): exploratory outcomes of a multicentre, phase 2, randomised controlled trial. Lancet Diabetes Endocrinol. 2019 Sep;7(9):673-683. doi: 10.1016/S221

[8] Pak, H.H., Haws, S.A., Green, C.L., Koller, M., Lavarias, M.T., Richardson, N.E., Yang, S.E., Dumas, S.N., Sonsalla, M., Bray, L., Johnson, M., Barnes, S., Darley-Usmar, V., Zhang, J., Yen, C.-L.E., Denu, J.M., Lamming, D.W.: Fasting drives the metabolic, molecular and geroprotective effects of a calorie-restricted diet in mice. Nature metabolism 3(10), 1327– 1341 (2021). doi: 10.1038/s42255-021-00466-9

[9] Bruss MD, Khambatta CF, Ruby MA, Aggarwal I, Hellerstein MK. Calorie restriction increases fatty acid synthesis and whole body fat oxidation rates. Am J Physiol Endocrinol Metab. 2010 Jan;298(1):E108-16. doi: 10.1152/ajpendo.00524.2009. Epub 2009 Nov 3. PMID: 19887594; PMCID: PMC4056782.

[10] Hahn, A. (2023). Lebensmittelchemie. Springer Spektrum, Berlin, Heidelberg. https://doi.org/10.1007/978-3-662-66925-9_2.

[11] Papadopoulou SK, Nikolaidis PT. Low-Carbohydrate Diet and Human Health. Nutrients. 2023 Apr 21;15(8):2004. doi: 10.3390/nu15082004. PMID: 37111222; PMCID: PMC10143153

[12] Hoffman JR, Falvo MJ. Protein - Which is Best? J Sports Sci Med. 2004 Sep 1;3(3):118-30. PMID: 24482589; PMCID: PMC3905294.

[13] Jo Y, Okazaki H, Moon YA, Zhao T (2016). "Regulation of Lipid Metabolism and Beyond". *International Journal of Endocrinology*. **2016**: 5415767. doi:10.1155/2016/5415767. PMC 4880713. PMID 27293434.

[14] Cho CH, Patel S, Rajbhandari P. Adipose tissue lipid metabolism: lipolysis. Curr Opin Genet Dev. 2023 Dec;83:102114. doi: 10.1016/j.gde.2023.102114. Epub 2023 Sep 20. PMID: 37738733.

[15] Gault CR, Obeid LM, Hannun YA (2010). "An Overview of Sphingolipid Metabolism: From Synthesis to Breakdown". *Sphingolipids as Signaling and Regulatory Molecules*. Advances in Experimental Medicine and Biology. Vol. 688. pp. 1–23. doi:10.1007/978-1-4419-6741-1_1. ISBN 978-1-4419-6740-4. PMC 3069696. PMID 20919643.

[16] Saely CH, Geiger K, Drexel H. Brown versus white adipose tissue: a mini-review. Gerontology. 2012;58(1):15-23. doi: 10.1159/000321319. Epub 2010 Dec 7. PMID: 21135534.

[17] Nagai M, Komiya H, Mori Y, Ohta T, Kasahara Y, Ikeda Y (May 2010). "Estimating visceral fat area by multifrequency bioelectrical impedance". *Diabetes Care*. **33** (5): 1077–1079. doi:10.2337/dc09-1099. PMC 2858179. PMID 20150289.

[18] Samuelson I, Vidal-Puig A (2020). "Studying Brown Adipose Tissue in a Human *in vitro* Context". *Frontiers in Endocrinology*. **11**: 629. doi:10.3389/fendo.2020.00629. PMC 7523498. PMID 33042008.

[19] Machado SA, Pasquarelli-do-Nascimento G, da Silva DS, Farias GR, de Oliveira Santos I, Baptista LB, Magalhães KG. Browning of the white adipose tissue regulation: new insights into nutritional and metabolic relevance in health and diseases. Nutr Metab (Lond). 2022 Sep 6;19(1):61. doi: 10.1186/s12986-022-00694-0. PMID: 36068578; PMCID: PMC9446768.

[20] Lo KA, Sun L (September 2013). "Turning WAT into BAT: a review on regulators controlling the browning of white adipocytes". *Bioscience Reports*. **33** (5): 711–19. doi:10.1042/BSR20130046. PMC 3764508. PMID 23895241.

[21] Yuan F, Jiang H, Yin H, Jiang X, Jiao F, Chen S, Ying H, Chen Y, Zhai Q, Guo F. Activation of GCN2/ATF4 signals in amygdalar PKC-δ neurons promotes WAT browning under leucine deprivation. Nat Commun. 2020 Jun 5;11(1):2847. doi: 10.1038/s41467-020-16662-2. PMID: 32504036; PMCID: PMC7275074.

[22] Fabbiano S, Suárez-Zamorano N, Rigo D, Veyrat-Durebex C, Stevanovic Dokic A, Colin DJ, Trajkovski M. Caloric Restriction Leads to Browning of White Adipose Tissue through Type 2 Immune Signaling. Cell Metab. 2016 Sep 13;24(3):434-446. doi: 10.1016/j.cmet.2016.07.023. Epub 2016 Aug 25. PMID: 27568549.

[23] Golbidi S, Daiber A, Korac B, Li H, Essop MF, Laher I. Health Benefits of Fasting and Caloric Restriction. Curr Diab Rep. 2017 Oct 23;17(12):123. doi: 10.1007/s11892-017-0951-7. PMID: 29063418.

[24] Demine S, Renard P, Arnould T. Mitochondrial Uncoupling: A Key Controller of Biological Processes in Physiology and Diseases. Cells. 2019 Jul 30;8(8):795. doi: 10.3390/cells8080795. PMID: 31366145; PMCID: PMC6721602.

[25] Ro SH, Jang Y, Bae J, Kim IM, Schaecher C, Shomo ZD. Autophagy in Adipocyte Browning: Emerging Drug Target for Intervention in Obesity. Front Physiol. 2019 Jan 28;10:22. doi: 10.3389/fphys.2019.00022. PMID: 30745879; PMCID: PMC6360992.

[26] Cao PJ, Jin YJ, Li ME, Zhou R, Yang MZ. PGC-1α may associated with the anti-obesity effect of taurine on rats induced by arcuate nucleus lesion. Nutr Neurosci. 2016;19(2):86-93. doi: 10.1179/1476830514Y.0000000153. Epub 2014 Sep 11. PMID: 25211138.

[27] Wen C, Li F, Zhang L, Duan Y, Guo Q, Wang W, He S, Li J, Yin Y. Taurine is Involved in Energy Metabolism in Muscles, Adipose Tissue, and the Liver. Mol Nutr Food Res. 2019 Jan;63(2):e1800536. doi: 10.1002/mnfr.201800536. Epub 2018 Oct 17. PMID: 30251429.

[28] Ide T, Kushiro M, Takahashi Y, Shinohara K, Cha S. mRNA expression of enzymes involved in taurine biosynthesis in rat adipose tissues. Metabolism. 2002 Sep;51(9):1191-7. doi: 10.1053/meta.2002.34036. PMID: 12200766.

[29] Bae M, Ahmed K, Yim JE. Beneficial Effects of Taurine on Metabolic Parameters in Animals and Humans. J Obes Metab Syndr. 2022 Jun 30;31(2):134-146. doi: 10.7570/jomes21088. Epub 2022 Jun 7. PMID: 35670160; PMCID: PMC9284575

[30] Ito T, Yoshikawa N, Ito H, Schaffer SW. Impact of taurine depletion on glucose control and insulin secretion in mice. J Pharmacol Sci. 2015 Sep;129(1):59-64. doi: 10.1016/j.jphs.2015.08.007. Epub 2015 Sep 1. PMID: 26382103.

[31] Hedrich, H.J.: The Laboratory Mouse, 2nd edn. Elsevier Science & Technology Books, Jordan Hill (2012).

[32] Gregor A, Panteva V, Bruckberger S, Aunon-Lopez A, Blahova S, Blahova V, et al. Energy and macronutrient restriction regulate bile acid homeostasis. J Nutr Biochem. 2023:109517;

[33] Duszka K, Ellero-Simatos S, Ow GS, Defernez M, Paramalingam E, Tett A, et al. Complementary intestinal mucosa and microbiota responses to caloric restriction. Sci Rep. 2018;8:11338.;

[34] Gregor AA-H, S. Malleier, M. Bruckberger, S. Séneca, J. Pjevac, P. Pignitter, P. Duszka, K. Fiber consumption stimulates the activity of microbial bile salt hydrolases. . Journal of Functional Foods. 2023;

[35] Gregor A, Pignitter M, Trajanoski S, Auernigg-Haselmaier S, Somoza V, Konig J, et al. Microbial contribution to the caloric restriction-triggered regulation of the intestinal levels of glutathione transferases, taurine, and bile acid. Gut Microbes. 2021;13:1992236;

[36] Kim KS, Jang MJ, Fang S, Yoon SG, Kim IY, Seong JK, et al. Anti-obesity effect of taurine through inhibition of adipogenesis in white fat tissue but not in brown fat tissue in a high-fat diet-induced obese mouse model. Amino Acids. 2019;51:245-54.

[37] Ferrecchia CE, Jensen K, Van Andel R. Intracage ammonia levels in static and individually ventilated cages housing C57BL/6 mice on 4 bedding substrates. J Am Assoc Lab Anim Sci. 2014;53:146-51.

[38] Gregor A, Fragner L, Trajanoski S, Li W, Sun X, Weckwerth W, et al. Cage bedding modifies metabolic and gut microbiota profiles in mouse studies applying dietary restriction. Sci Rep. 2020;10:20835.

[39] Drew JE, Reichardt N, Williams LM, Mayer CD, Walker AW, Farquharson AJ, et al. Dietary fibers inhibit obesity in mice, but host responses in the cecum and liver appear unrelated to fiber-specific changes in cecal bacterial taxonomic composition. Sci Rep. 2018;8:15566.

[40] Zou J, Chassaing B, Singh V, Pellizzon M, Ricci M, Fythe MD, et al. Fiber-Mediated Nourishment of Gut Microbiota Protects against Diet-Induced Obesity by Restoring IL-22-Mediated Colonic Health. Cell Host Microbe. 2018;23:41-53 e4.

[41] Desai MS, Seekatz AM, Koropatkin NM, Kamada N, Hickey CA, Wolter M, et al. A Dietary Fiber-Deprived Gut Microbiota Degrades the Colonic Mucus Barrier and Enhances Pathogen Susceptibility. Cell. 2016;167:1339-53 e21.

[42] Macfarlane S, Macfarlane GT. Regulation of short-chain fatty acid production. The Proceedings of the Nutrition Society. 2003;62:67-72.

[43] Weitkunat K, Schumann S, Petzke KJ, Blaut M, Loh G, Klaus S. Effects of dietary inulin on bacterial growth, short-chain fatty acid production and hepatic lipid metabolism in gnotobiotic mice. J Nutr Biochem. 2015;26:929-37.

[44] Chassaing B, Miles-Brown J, Pellizzon M, Ulman E, Ricci M, Zhang L, et al. Lack of soluble fiber drives diet-induced adiposity in mice. Am J Physiol Gastrointest Liver Physiol. 2015;309:G528-41.

[45] Zhang M, Bi LF, Fang JH, Su XL, Da GL, Kuwamori T, et al. Beneficial effects of taurine on serum lipids in overweight or obese non-diabetic subjects. Amino Acids. 2004;26:267-71.

[46] Murakami S. The physiological and pathophysiological roles of taurine in adipose tissue in relation to obesity. Life Sci. 2017;186:80-6.

[47] Haidari F, Asadi M, Mohammadi-Asl J, Ahmadi-Angali K. Effect of weight-loss diet combined with taurine supplementation on body composition and some biochemical markers in obese women: a randomized clinical trial. Amino Acids. 2020;52:1115-24.

[48] Tsuboyama-Kasaoka N, Shozawa C, Sano K, Kamei Y, Kasaoka S, Hosokawa Y, et al. Taurine (2-aminoethanesulfonic acid) deficiency creates a vicious circle promoting obesity. Endocrinology. 2006;147:3276-84.

[49] Wang Z, Ohata Y, Watanabe Y, Yuan Y, Yoshii Y, Kondo Y, et al. Taurine Improves Lipid Metabolism and Increases Resistance to Oxidative Stress. J Nutr Sci Vitaminol (Tokyo). 2020;66:347-56.

[50] Hivert MF, Sullivan LM, Fox CS, Nathan DM, D'Agostino RB, Sr., Wilson PW, et al. Associations of adiponectin, resistin, and tumor necrosis factor-alpha with insulin resistance. J Clin Endocrinol Metab. 2008;93:3165-72.

[51] Mendes de Oliveira E, Silva JC, Ascar TP, Sandri S, Marchi AF, Migliorini S, et al. Acute Inflammation Is a Predisposing Factor for Weight Gain and Insulin Resistance. Pharmaceutics. 2022;14.

[52] Younis NS, Ghanim AMH, Elmorsy MA, Metwaly HA. Taurine ameliorates thioacetamide induced liver fibrosis in rats via modulation of toll like receptor 4/nuclear factor kappa B signaling pathway. Sci Rep. 2021;11:12296.

[53] Lin CJ, Chiu CC, Chen YC, Chen ML, Hsu TC, Tzang BS. Taurine Attenuates Hepatic Inflammation in Chronic Alcohol-Fed Rats Through Inhibition of TLR4/MyD88 Signaling. J Med Food. 2015;18:1291-8.

[54] Lin S, Hirai S, Yamaguchi Y, Goto T, Takahashi N, Tani F, et al. Taurine improves obesity-induced inflammatory responses and modulates the unbalanced phenotype of adipose tissue macrophages. Mol Nutr Food Res. 2013;57:2155-65.

[55] Kim C, Cha YN. Taurine chloramine produced from taurine under inflammation provides anti-inflammatory and cytoprotective effects. Amino Acids. 2014;46:89-100.